Shoreline Response for a Reef Ball ™ Submerged Breakwater System Offshore of Grand Cayman Island

By

Dana Suzanne Arnouil

Bachelor of Science
Ocean Engineering
Florida Institute of Technology
2006

A thesis submitted to
Florida Institute of Technology
in partial fulfillment of the requirements
for the degree of

Master of Science
in
Ocean Engineering

Melbourne, Florida
August, 2008

Shoreline Response for a Reef Ball ™ Submerged Breakwater System Offshore of Grand Cayman Island

A thesis by
Dana Suzanne Arnouil

Approved as to style and content by:

_____

Lee E. Harris, Ph.D.,P.E., Committee Chair
Associate Professor, Ocean Engineering
Department of Marine and Environmental Systems

_____

Steven M. Jachec, Ph.D.,P.E., Committee Member
Assistant Professor, Ocean Engineering
Department of Marine and Environmental Systems

_____

Ralph V. Locurcio, M.S.E.,P.E., Committee Member
Professor, Civil Engineering
Department of Civil Engineering

_____

George A. Maul, Ph.D., Program Chair
Professor, Oceanography
Department of Marine and Environmental Systems

Abstract

Shoreline Response for a Reef Ball ™ Submerged Breakwater System Offshore of Grand Cayman Island

Author

Dana S. Arnouil

Principal Advisor

Lee E. Harris, Ph.D., P.E.

As coastal development in the Cayman Islands increases, the importance of beach erosion continues to increase. One location that experiences greater than normal erosion is the stretch of beach adjacent to the Marriott Hotel, located on the southern end of Seven Mile Beach, in Grand Cayman, B.W.I. In order to stabilize the eroded beach, a submerged breakwater system was constructed approximately 170 feet offshore. The breakwater system consists of 232 Reef Ball artificial reef units, 200 of which were installed in the fall of 2002, and 32 in the fall of 2005. Following the breakwater extension in the fall of 2005, approximately 6,000 cubic yards of beach fill were placed along 1,000 feet in the southern Seven Mile Beach area, with approximately 1,900 cubic yards placed in front of the Marriott.

To provide a basis for examining the effects of this breakwater system, a field monitoring program was conducted, which included the collection of beach

profile surveys, beach width measurements, and ground and aerial photographic images. These data provided information to analyze the behavior of the beach and shoreline response, including shoreline, cross-shore, and volumetric changes, in addition to determining the expected wave transmission and sand transport leeward of the breakwater.

In November 2002, prior to the installation of the breakwater system, the shoreline in front of the Marriott had retreated to the seawall, with waves scouring underneath the seawall. Since the installation of the submerged breakwater system the beach width and volume of sand have substantially increased. The beach width varied seasonally 25 to 70 feet, compared to 0 to 30 feet before installation. Four years after the completion of the project, the average beach width reached 72 feet. Wave transmission analysis, based on empirical equations, showed a wave height reduction of at least 60%. Under most non-storm conditions, sediment leeward of the breakwater remains stable, and has allowed a salient to build up in front of the Marriott Hotel.

Table of Contents

List of Figures

List of Tables

List of Symbols and Abbreviations

Symbol	Definition	Units
A	Cross-sectional area of breakwater	ft^2
B	Breakwater crest width	ft
d	Depth at toe of structure	ft
d_s	particle diameter	ft
D_{n50}	Nominal diameter of stone	ft
F	Freeboard	ft
g	Acceleration due to gravity	ft/s^2
h	Height of breakwater	ft
H_i	Incident wave height	ft
H_t	Transmitted wave height	ft
k	Wave number	N/A
K_t	Wave transmission coefficient	N/A
L	Wave length	ft
L_s	Length of breakwater structure	ft
MWL	Mean water level	ft
R_*	Grain Reynolds number	N/A
SWL	Still water level	ft
T	Wave period	s
U	Horizontal water particle velocity	ft/s
u_*	Shear velocity	ft/s
V	Volume	cyd/ft
X	Distance from the undisturbed shoreline	ft

κ	Breaker index	
ρ_s	Grain density	lb/ft^3
ρ_f	Fluid density	lb/ft^3
τ_*	Shields parameter	N/A
τ_o	Bed shear stress	$lb/ft\text{-}s^2$
$(\tau_o)_c$	Critical shear stress	$lb/ft\text{-}s^2$
γ_s	Particle specific weight	$slugs/ft^3$
γ	Fluid specific weight	$slugs/ft^3$
υ	Kinematic viscosity	ft^2/s^2
μ	Dynamic viscosity	lb/ft s

Acknowledgements

I would like to thank the following people: Dr. Harris for providing me with guidance, support, and information for this study; my parents, for financial and emotional support; my committee members, Dr. Jachec and General Locurcio for their help and support; Todd Barber and the Reef Ball Foundation, Inc. for giving me the opportunity to volunteer with the Reef Ball Foundation on this breakwater project; Tim Austin (Cayman Islands Department of Environment) for providing me with useful information about the project. I would also like to thank Eric Mitchell, Aurelie Moulin, Pamela Christian, Joe Morrow, Adam Priest, Chris Flanary, and Kevin Hodgens for their help along the way.

1 Introduction

The coastline, dividing land and sea, has always played a significant role in human activities. Humans have been building along the coast for centuries. Major cities are built along the coast; tourism and recreation bring in revenue; ports and harbors serve as bases for trade and military use. Coastal development continues to increase, especially in the form of residential and commercial properties, where over 50 percent of the U.S. population now lives within 50 miles of the coastline (Dean and Dalrymple, 2002). Natural coastal processes are impact efforts to maintain coastal development (Dean and Dalrymple, 2002), typically resulting in coastal erosion.

There are many factors that can contribute to long term coastal erosion including (Silvester and Hsu, 1997 and Pilarczyk and Zeilder, 1996):

- Obliquely incident waves, storm events, extreme tides or currents, sea level rise
- Disrupting or changing sediment transport, natural or man-induced
- Loss of sand from aeolian (wind) transport of sediments to upland areas, lagoons, inlets, etc., or excavated for construction reasons
- Elimination of sources of organic sediments as a result of water pollution

Many methods have been developed to prevent or control erosion, as itemized in Table 1. Protection design should be effective (practical for the environment and consumer) and efficient (cost-effective and resourceful) (Schiererck, 2001).

Table 1. Alternative Solutions for Coastal Erosion and Protection.
(U.S. Army Corps of Engineers, 2006a)

Type of Structure	Objective	Principal Function
Sea dike	Prevent/lessen flooding by the sea of low-lying land area	Separation of shoreline from hinterland by a high impermeable structure
Seawall	Protect land/structures from flooding and overtopping	Reinforcement of part of the beach profile
Revetment	Protect the shoreline against erosion	Reinforcement of part of the beach profile
Bulkhead	Retain soil and prevent sliding of the land behind	Reinforcement of the soil bank
Groin	Prevent beach erosion	Reduction of longshore transport of sediment
Breakwater	Shelter harbor basins, harbor entrances, and water intakes against waves and currents	Dissipation of wave energy and/or reflection of wave energy back into the sea
Detached breakwater	Prevent beach erosion	Reduction of wave heights in the lee of the structure and reduction of longshore transport of sediment
Reef breakwater	Prevent beach erosion	Reduction of wave heights at the shore
Floating breakwater	Shelter harbor basins and mooring areas against short-period waves	Reduction of wave heights by reflection and attenuation
Submerged sill	Prevent beach erosion	Retard offshore movement of sediment
Beach drain	Prevent beach erosion	Accumulation of beach material on the drained portion of beach
Beach nourishment and dune construction	Prevent beach erosion and protect against flooding	Artificial fill of beach and dune material to be eroded by waves and currents in lieu of natural supply
Jetty	Stabilize navigation channels at river mouths and tidal inlets	Confine streams and tidal flow. Protect against storm water and crosscurrents

Many times these methods only work for short periods of time or can actually exacerbate the problem. Seawalls can be effective at reducing erosion landward of the structure but may cause erosion in the front of the structure due to wave reflection and scouring, resulting in a steeper seabed profile (U.S. Army Corps of Engineers, 2006a). Many times seawalls are used in combination with groins and/or beach nourishment. Groins, shore-perpendicular structures that impede longshore sediment transport, cause accretion on the updrift side of the structure and erosion on the downdrift side (Hanson and Kraus, 2001). Therefore, typical installation requires a series of multiple groins. Beach nourishment, recognized as a soft option for coastal stabilization, shows quick results, but are expensive and need to be renourished periodically.

Breakwaters are also commonly used for shoreline stabilization. These structures can be designed to reduce erosion on an existing beach, support sedimentation to form a new beach, protect against storm damage, or help to prolong a beach nourishment (Pilarczyk and Zeilder, 1996). Breakwaters can be shore-attached or detached, emergent or submerged, shore-parallel or oblique (Pilarczyk and Zeilder, 1996). The primary purpose of breakwaters are to dissipate wave energy and modify wave and current fields in the lee (landward) of the breakwater. Emergent, or subaerial, breakwaters are effective at controlling erosion but can have an adverse impact on beach amenity and aesthetics.

One of the best ways to protect a beach is to emulate natural defense mechanisms. Erosion and accretion are natural and seasonal processes of beach dynamics. How the beach responds to this cyclic process is a good example of how the beach itself is it own best protection. During storm activity with large short period waves, sand is removed from the beach, constructing an offshore bar that forces large waves to break and dissipate before reaching the shore. Once smaller longer period waves return, the sand moves back onshore and the beach and dune are rebuilt to prepare for the next storm attack. Offshore reefs have been known to

provide natural shoreline stabilization by supplying that nearshore bar necessary for wave dissipation. Dissipation is due to a combination of frictional dissipation and wave breaking (Lowe *et. al.*, 2005). Submerged breakwaters essentially act in the same manner. Submerged structures allow smaller waves to be transmitted and attenuate only larger waves.

One location utilizing submerged breakwaters for erosion control is in front of the Marriott Hotel, located on the southern part of Seven Mile Beach, in Grand Cayman, B.W.I. In an effort to stabilize the shoreline, the Marriott Hotel installed a submerged breakwater consisting of Reef Ball artificial reef units. Erosion has been a concern along Seven Mile Beach, located on the western side of Grand Cayman Island. Grand Cayman is located 480 miles south of Miami in the Caribbean Sea and is the largest (78 square miles) of the three islands that make up the Cayman Islands, shown in Figure 1. Conserving the beaches in Grand Cayman is a high priority for the Cayman Island Government since tourism accounts for about 70% of GDP (Gross Domestic Product) and 75 % of foreign currency earnings (The World Factbook, 2008). Seven Mile Beach is Grand Cayman's primary tourist attraction and is part of the main stretch of developed coastline (Figure 2). In 2003, an interim report provided by the Cayman Island Beach Review and Assessment Committee, outlined various projected causes and proposed solutions of the erosion problem.

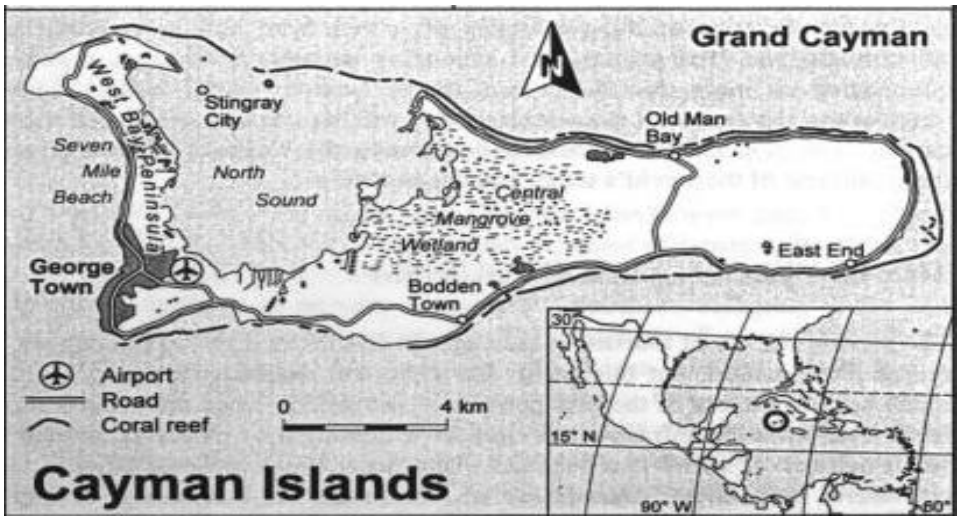

Figure 1. Grand Cayman location map.
(Weaver, 2003)

Figure 2. Location of Seven Mile Beach and the Marriott Hotel.
(Photo Courtesy of Google Earth)

The objective of this study was to examine the effect of the Marriott breakwater system in terms of shoreline response. Periodic monitoring was performed after the installation, but a detailed analysis has not been completed to determine the net result of this Reef Ball breakwater system. In order to determine the impact of the structure, survey data and aerial imagery were analyzed. The procedure used to describe the behavior of the shoreline is based on shoreline and volumetric changes, which can describe the overall and local performance of the breakwater. The expected wave transmission over the structure was also calculated and compared using different empirical equations. Analyzing shoreline and volume change patterns over time is very useful in determining the collective effects of natural processes and human influences. For the Marriott Hotel, the shoreline provides natural protection from waves and a recreational area for hotel guest. Estimating the transmitted wave heights in the lee of the structure indicates the level of protection provided by the breakwater. By evaluating how this breakwater affected the shoreline, modifications can be planned and future breakwater designs can be improved.

2 Background and Review of Literature

2.1 Submerged Breakwaters for Shore Protection

The use of submerged breakwaters for shore protection has increased in recent years. Submerged breakwaters have the potential to provide beach protection without destroying or reducing beach amenity or aesthetics (Ranasinghe and Turner, 2006).

Submerged structures can have effects similar as that of natural offshore reefs, creating salients and tombolos (build up of sand) of sediment deposits in their lee (Black and Andrews, 2001), suggesting a possible application for beach protection (Pilarczyk and Zeilder, 1996). Submerged breakwaters, when properly designed, allow partial wave attenuation to help protect the beach. As waves approach these structures, they break, losing energy as they pass over the crest of the structure. The decrease in wave energy and modification of nearshore currents can support sediment deposition at the shoreline without disrupting existing coastal processes. Ranasinghe and Turner (2006) present instances where submerged breakwaters were both successful and unsuccessful for erosion mitigation, and they found mixed results on the shoreline response of such structures. The shoreline response to submerged breakwaters is not fully understood, and techniques used to predict shoreline response to emergent structures are not acceptable for submerged breakwater designs. Therefore, the characteristics affecting shoreline response to submerged structures must be carefully examined (Ranasinghe and Turner, 2006).

Various studies have verified the use of submerged breakwaters for shore protection and stabilization indirectly with the help of understanding wave and sediment dynamics. Black and Mead (2001) discuss how submerged breakwaters can help align waves to be more "shore-parallel" with the concept of wave rotation. Black and Andrews (2001) found that salient growth in the lee of the breakwater leads to enhanced shoreline stability and protection. This trend occurs because the breakwater will diminish wave height in its lee, which reduces the wave's ability to transport sand. Meanwhile, sediment will build up in the lee of the breakwater due to the longshore current. Figure 3 shows an idealized shoreline response to a submerged breakwater during obliquely incident waves.

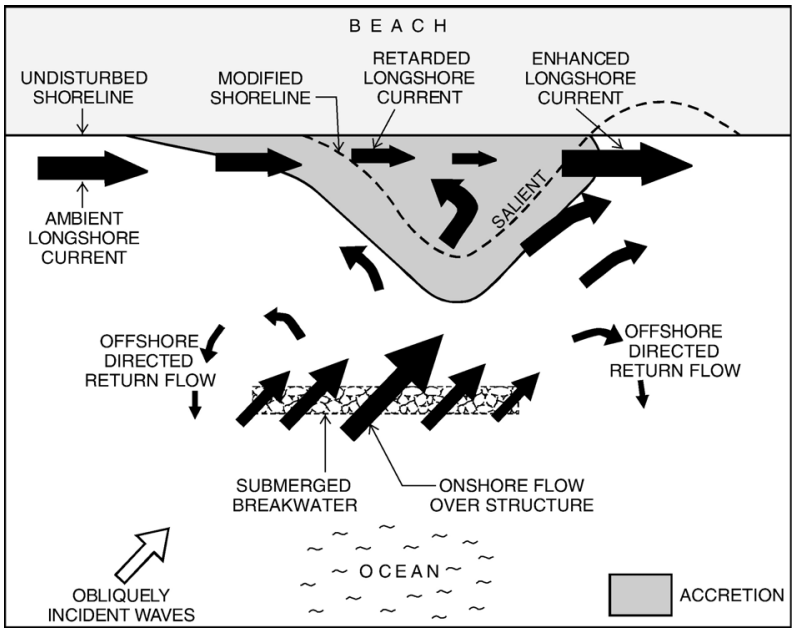

Figure 3. Nearshore circulation and accretion patterns in response to a submerged breakwater under oblique wave incidence.
(Ranasinghe and Turner, 2005)

2.1.1 Negative Impacts

There are examples of submerged breakwaters producing adverse effects. Dean *et al.* (1997) conducted an extensive monitoring study of a submerged breakwater (known as the PEP reef) in West Palm Beach, Florida. According to this monitoring effort, erosion in the lee was twice as much as the background erosion in the area. The reefs were considered a failure and were removed and groins were constructed. Dean *et al.* (1997) attributed this failure to inadequate wave attenuation, "ponding" occurring leeward of the structure, and considerable settlement of the reef. Another monitoring study was conducted by Douglass and Weggel (1986) of a submerged breakwater that was anticipated to hold a beach fill in Delaware Bay. After four years of periodic beach profile surveys, a salient in the lee of the breakwater initially formed after the beach fill, but in the end the entire volume of the fill vanished. The net longshore sediment transport resulting from oblique wave incidence is believed to be responsible for erosion in this case. These studies explain the importance addressing design considerations and knowledge of how submerged breakwaters perform under oblique incident waves (Silvester and Hsu, 1997).

2.1.2 Breakwater Design Considerations

The design characteristics of a breakwater structure are important in determining how the structure will impact the shoreline. Studies on the effect of design characteristics, in and out of the laboratory, have increased over the years. Some of these design parameters for a submerged breakwater are shown in Figure 4.

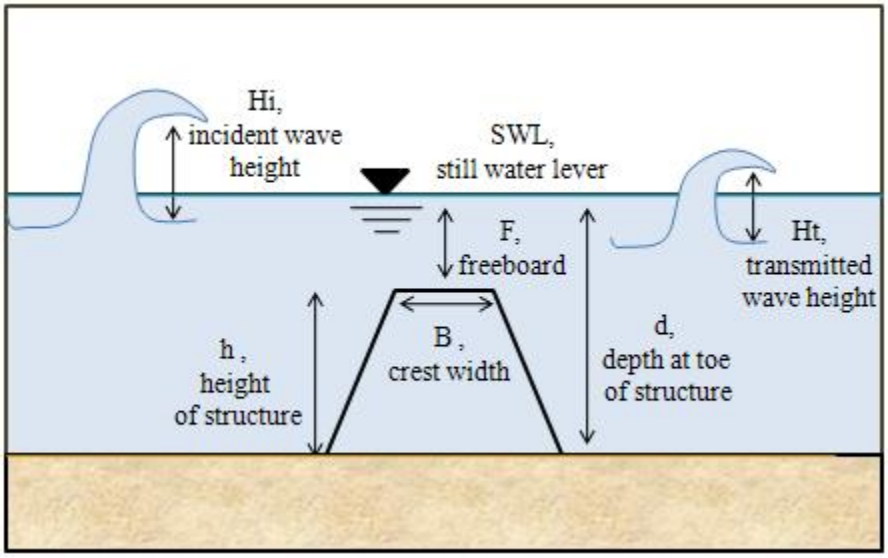

Figure 4. Parameters for a submerged breakwater.

These characteristics include:

- length of the breakwater (Black and Andrews, 2001)
- crest width (Ting *et al.,* 2004)
- distance and position offshore (Black and Mead, 2001)
- gap in between breakwaters (Birben *et al.,* 2005)
- the size and height of structure (Ranasinghe *et al.*, 2006)
- degree of emergence or submergence (Harris, 1996)
- breakwater relative crest height (Harris, 1996)

The degree of submergence can be represented by three dimensionless ratios:

- the degree of submergence ,

$$\frac{d}{h}, \tag{1}$$

- the relative structure height,

$$\frac{h}{d}, \tag{2}$$

- the relative freeboard to water depth ratio,

$$\frac{F}{d} = \frac{h-d}{d} = \frac{h}{d-1}, \quad (3)$$

The breakwater relative crest height can also be represented by the following ratio, which includes wave height:

$$\frac{F}{H} = \frac{h-d}{H} = \frac{h}{H} - \frac{d}{H}, \quad (4)$$

where F is the freeboard, h is the height of the structure, d is the water depth at the toe of the structure, and H is the incident wave height.

The importance of the length of the breakwater, L_s, and its distance from the undisturbed shoreline, X, is seen in Table 2. The ratio of L_s /X determines the type of formation that will occur (tombolo, salient, or non-deposited).

The height of the breakwater, or submergence level, is another important design characteristic to be considered. If the breakwater height is too small, incoming waves will not "touch" the breakwater surface, resulting in ineffective wave attenuation (Armono and Hall, 2003). Relative structure height should be 60-80% for optimum effectiveness (Harris, 1996). Armono and Hall (2003) showed that "for low submerged depths, (i.e., the breakwater height is more than 70% of water depth) the effect of breakwater width (or reef proportion) is noticeable."

Crest width has also been shown to affect the wave transmission properties of a submerged breakwater. Stauble and Tabar (2003) showed that narrow-crested designs, such as the P.E.P. reefs, have shown to have limited their effectiveness in wave attenuation and a "… steeper landward facing slope experienced scour on the landward base."

Table 2. Type of shoreline formation for the ratio L_s/X.

Type of Formation	Ratio	Notes	Reference
Tombolo	$L_s/X > 0.6$	offshore reefs	(Black and Andrews, 2001)
	$L_s/X = 1.5$ to 2	single breakwater	(Dally and Pope, 1986)
	$L_s/X = 1.5$	multiple breakwater (L < G < B)	(Dally and Pope, 1986)
	$L_s/X => 1.0$	single breakwater	(Suh and Dalrymple, 1987)
	$G*X/ L_s^2 = 0.5$	multiple breakwaters	(Suh and Dalrymple, 1987)
	$L_s/X >$ (1.0 to1.5)/(1-K_t)	submerged breakwaters	(Pilarczyk, 2003)
Salient	$L_s/X < 2$	offshore reefs	(Black and Andrews, 2001)
	$L_s/X = 0.67$ to 1.5		(Dally and Pope, 1986)
	$L_s/X = 0.5$-1.0		(Shore Protection Manual, 1984)
	$L_s/X < 1/(1-K_t)$	submerged breakwaters	(Pilarczyk, 2003)
	$G*X/ L_s^2 = 0.5(1-K_t)$	multiple submerged breakwaters	(Pilarczyk, 2003)
Non-depositional conditions	$L_s/X < 1$	offshore reefs	(Black and Andrews, 2001)
	$L_s/X < 0.5$		(Nir, 1982)

Other considerations that must be taken into account when designing submerged breakwaters are stability, scour, settlement, sliding and overturning. Breakwaters need to be designed to "withstand the breaking wave forces, wave-induced currents and scour that occur in the surf zone" (Harris, 2006). Structural design aspects of submerged structures are described in a number of publications (Ahrens, 1987; Pilarczyk and Zeidler, 1996; Roehl, 1997, etc.). Roehl (1997) derived an equation to determine the stability of manufactured artificial reefs, including reef ball units. From this equation he developed stability curves for different wave heights and periods to determine the required minimum weight for

stability for each unit. Yuan and Tao (2003) also did a study on the wave forces on semicircular breakwater units. They concluded that with semicircular breakwaters:

1. No overturning moments are generated by wave pressure, because the pressure passes through the center of the semicircular shape.
2. Due to the hollowness of the semicircular structure, the vertical force acting on the soil is small and "almost uniformly distributed", preventing settlement even in soft soil foundation
3. The lateral force acting is smaller on a semicircular breakwater than a vertical breakwater of the same height, improving stability against sliding
4. Since semicircular breakwaters are prefabricated and not constructed on site, they can endure large waves instantly after installation

2.1.3 Wave Transmission Models

The primary purpose of breakwaters is to dissipate wave energy. By design, the structure may allow a certain amount of wave energy to transmit past the breakwater. Shoreline response to breakwaters derives partly from the attenuation of the incident wave. The greater submergence of a breakwater, the less the wave impacts the structure, and the less effective it is for wave attenuation. The parameter used to measure the effectiveness of a breakwater in terms of wave attenuation is the transmission coefficient,

$$K_t = \frac{H_t}{H_i}, \tag{5}$$

where K_t is the wave transmission coefficient, H_t is the transmitted wave height on the lee of the structure, and H_i is the incident wave height on the seaward side of the structure (U.S. Army Corps of Engineers, 1984). The larger the wave transmission coefficient, the less the wave is attenuated.

An alternative method for defining the wave transmission coefficient is defined by Ahrens (1987), which is the ratio of the transmitted wave height, H_t, to the wave height which would be observed at the same location without the breakwater, H_c,

$$K_t = \frac{H_t}{H_c}, \tag{6}$$

This ratio is defined to account for wave energy losses occurring between the incident and transmitted gages in the absence of a breakwater (Ahrens, 1987).

Many empirical equations are available for predicting transmission coefficients for submerged breakwaters. Growing interest in using submerged breakwaters for shoreline stabilization requires correct models and relationships for predicting wave transmission. These equations are valuable for estimating transmitted wave heights in the lee of the structure, to give an idea of the level of protection provided by the breakwater.

Ahrens (1987) offers an empirical formula for reef breakwaters with the ratio of the freeboard to the incident wave height less than one as,

$$K_t = \frac{1}{1 + \left(\frac{h}{d}\right)^{1.188} \left(\frac{A}{dL}\right)^{0.261} \exp\left(0.529\left(\frac{F}{H}\right) + 0.00551\left(\frac{A^{3/2}}{D_{n50}^2 L}\right)\right)}, \tag{7}$$

where d is the water depth, h is the height of the structure, A is the cross-sectional area of the breakwater, L is the wavelength, D_{n50} is the nominal diameter of stone, H is the wave height, and F is the freeboard. The term D_{n50} is used for rubble mound breakwaters and does not pertain to singular units which do not consist of stones.

Seabrook and Hall (1998) developed an equation for wave transmission at submerged rubble mound breakwaters from physical modeling tests of submerged

breakwaters, using various freeboard, crest widths, water depths, and incident wave conditions:

$$K_t = 1 - \left(e^{0.65\left(\frac{F}{H}\right) - 1.09\left(\frac{H}{B}\right)} - 0.047\left(\frac{BF}{LD_{n50}}\right) + 0.067\left(\frac{FH}{BD_{n50}}\right)\right) \quad (8)$$

Friebel and Harris (2004) derived a new empirical wave transmission formula from data collected from five physical model studies, defined as:

$$K_t = -0.4969e^{\left(\frac{F}{H}\right)} - 0.0292\frac{B}{d} - 0.4257\frac{h}{d} - 0.0696\ln\left(\frac{B}{L}\right) + 0.1359\frac{F}{B} + 1.0905\,, \quad (9)$$

The data sets used the Friebel and Harris (2004) analysis were provided from previous studies by Seelig (1980), Daemrich and Kahle (1985), Van der Meer (1988), Daemen (1991), and Seabrook and Hall (1998), excluding the data set from Ahrens (1987) due to variations in structure crest heights during testing. Friebel and Harris (2004) results verify that the transmission coefficient depends greatly on the ratio of freeboard to incident wave height, $\frac{F}{H}$, relative width, $\frac{B}{d}$, and relative structure height, $\frac{h}{d}$. The authors recommend application of this equation within the following range of design parameters: $\frac{\mathrm{F}}{\mathrm{H}}$ = -8.696~0.000, $\frac{B}{d}$ = 0.286~8.750, $\frac{h}{d}$ = 0.440~1.000, $\frac{B}{L}$ = 0.024~1.890, and $\frac{F}{B}$ = -1.050~0.000.

Armono and Hall (2003) developed a mathematical model for wave transmission based on two dimensional tests using regular and irregular water over perforated hollow hemispherical shape artificial reefs (HSAR), which included the use of Reef Balls. The following equation was found to be a satisfactory description of the wave transmission through HSAR breakwaters:

$$K_t = 1.616 - 31.322\frac{H_i}{gT^2} - 1.099\frac{h}{d} + 0.265\frac{h}{B}\,, \quad (10)$$

where $\frac{H_i}{gT^2}$ is the wave steepness, T= wave period, $\frac{h}{d}$ is the depth of submergence, and $\frac{h}{B}$ is the reef proportion. This equation provides a good estimate for K_t for the type of structure tested within the range of parameters: $\frac{H_i}{gT^2}$ = 0.001~0.015, $\frac{h}{d}$ = 0.7~1, and $\frac{h}{B}$ = 0.35 ~ 0.583.

2.2 Reef Ball Breakwaters

Advantages of using submerged breakwaters are their versatility to not only improve shoreline protection, but also to enhance local surfing conditions (Ranasinghe and Turner, 2005) and as artificial reefs, "providing habitat for benthic and pelagic flora and fauna" (Harris, 2006). A large amount of research has been done supporting the benefits of using artificial reefs as submerged breakwaters. Black (2000) explains that offshore reefs are described by three essential characteristics expressed by the acronym MOA (Multi-purpose, offshore, and adjustable). With submerged breakwaters as artificial reefs, the visual amenity of the beach is not impaired, and recreational and public amenities can be incorporated through surfing, diving, sheltered swimming, fishing and marine habitat with low environmental impact (Black, 2000).

One type of artificial reef unit recently used for submerged breakwaters is a permeable, hollow cement hemisphere known as Reef Ball™, shown in Figure 5. Reef Balls were originally designed as artificial reefs for biological enhancement, but uses have expanded to many other applications including shoreline stabilization, oyster growth, mangrove rehabilitation, and as marina protection (Reef Beach Company, Ltd., 2007). Precht (2006) states that "due to the combination of creativity and aptitude for ecological restoration, Reef Balls are increasingly popular with the marine tourism throughout the world."

Figure 5. Reef Ball unit installed off Grand Cayman Island.
(Photo courtesy of Lee Harris)

Reef Balls offer flexibility, as they come in various sizes, shapes, and designs and can be removed or transferred if needed. They are easy to install and can be constructed locally, even on site. Costs depend on the local prices for concrete, rock, sand, equipment, and boat time for deployment (Reef Beach Company, Ltd., 2007).

The molds are pre-fabricated to the desired size with inflated buoys and ballsinside to produce the various holes throughout the Reef Ball. Additives, such as microsilica, are added to the concrete to "… increase strength and workability plus decrease the pH of the concrete to that of marine environment" (Harris, 2003a). The concrete is poured into the molds, and then when cured, the units are transported and deployed as early as 48 hours later.

Reef Balls can be transported on a barge and deployed individually using a crane (Figure 6), or rolled down the beach or backed into the ocean with a trailer. Lift bags can be used to float the units to the site for precise placement in desired

locations. Figure 7 shows an example Reef Ball Breakwater after installation in Grand Cayman Island.

Figure 6. Reef Balls being deployed from a barge.
(Photo courtesy of Lee Harris)

Figure 7. Reef Ball Breakwater after installation in Grand Cayman Island.
(Photo courtesy of Lee Harris)

2.3 Shoreline Analysis

Shoreline analysis of trends and variability is important for many coastal engineering applications, especially when the shoreline evolution is altered by installing a submerged breakwater. Periodic beach and nearshore profiles survey data can be used to analyze shoreline changes, in addition to volumetric changes and sediment transport. A tidal-based shoreline are determined shoreline can be detected by interpolating between a series of cross-shore beach profiles (Boak and Turner, 2005). Aerial photographs can also be used to analyze shoreline changes. Large areas in short amount of time and inaccessible terrain can be surveyed by aircraft (Gorman *et. al.,* 1998) Shoreline change mapping can reveal details on:

- Long and short term advance or retreat of the shore
- Longshore movement of sediments
- Storm Impacts
- Human impacts
- Biological conditions

Factors affecting potential errors associated with field surveys and aerial photographs are location, quality and quantity of control points, interpretation of datum, surveying standards, aircraft tilt, pitch, and altitude change, topographic relief, and film prints versus contact prints (Gorman *et. al.,* 1998).

To effectively analyze shoreline changes from field surveys and aerial photographs a consistent and practical definition of the "shoreline" is necessary. In a study done by Boak and Turner (2005) different methods of indicating the shoreline are described, making the issue of shoreline definition and detection apparent. Many possible indicators are used to monitor historical changes in the shoreline. Shoreline indicators include:

- mean high or low water line
- actual high of low water line

- wet/dry line
- mean water level
- beach toe
- vegetation line

These indicators may include problems such as the position being affected by wind, wave, run-up, and tide conditions, or vegetation not being present, etc. All data must be corrected to a common datum, scale, projection, and coordinate system before being compared.

2.4 Sediment Transport

Understanding the characteristics of sediment transport is important for many coastal engineering applications, including prediction of the effects of coastal structures. The motion of a particle of sand is caused by forces acting on the particle, as shown in Figure 8. The drag force, F_D, acts in the direction of the flow, the lift force, F_L, acts perpendicularly away from the sediment bed, and the weight, W_s, acts downward. These forces are expressed as,

$$F_D = \frac{1}{2}\rho C_D U^2 A_p \tag{11}$$

$$F_L = \frac{1}{2}\rho C_L U^2 A_p \tag{12}$$

$$W_S = (\rho_s - \rho) g V_p \tag{13}$$

where U is the horizontal flow velocity, C_D and C_L are the drag and lift coefficients that depend on the flow Reynolds number, A_p (= $\pi d^2/4$) and V_p(= $\pi d^3/6$) are the particle's projected area and volume (assuming a spherical particle with a diameter, d_s) and the term (ρ_s-ρ)g is the submerged specific weight of the sediment.

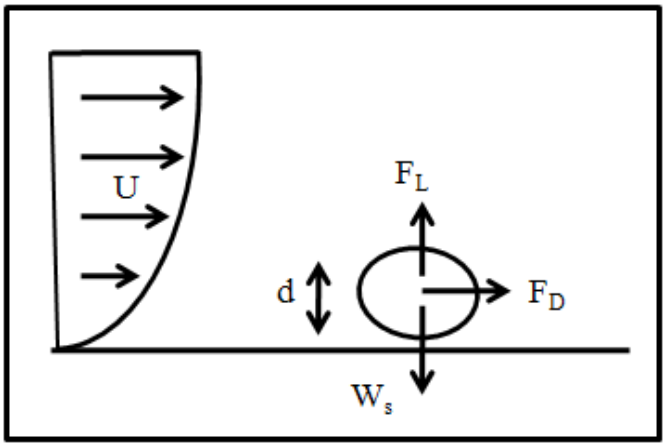

Figure 8. Forces acting on a grain resting on the bed.
(Adapted from Dean and Dalrymple, 2002)

Most incipient motion criteria are derived from either a shear stress or a velocity method. Although velocity has been used previously for predicting sediment transport, Shields (1936) relationship between dimensionless shear stress known as the Shields parameter, τ_*, and grain Reynolds number, R_*, is now widely accepted as a more consistent predictor (U.S. Army Corps of Engineers, 1995). The grain Reynolds number and Shields parameter are defined as:

$$R^* = \frac{u_* d_s}{\upsilon} = d\frac{(\tau_o/\rho_f)^{1/2}}{\nu} \tag{14}$$

$$\tau_* = \frac{\tau_o}{(\gamma_s - \gamma)d} = \frac{\tau_o}{d\gamma\left((\rho_s/\rho_f) - 1\right)} \tag{15}$$

where τ_o = bed shear stress
γ_s = particle specific weight
γ = fluid specific weight
ρ_s= particle density
ρ_f = fluid density
ν = kinematic viscosity of the fluid
g = acceleration of gravity
d_s = particle diameter
u_* = shear velocity

The Shields parameter and grain Reynolds number are dimensionless; therefore, any consistent units of measurement can be used in their calculation. A particle will move when the shear stress acting on it is greater than the resistance of the particle to movement. Critical shear stress, $(\tau_*)_c$, is the shear stress required to initiate sediment movement. Figure 9 shows the experimental results obtained by Shields at incipient motion. For points above the curve, the sediments are transported in the form of bed-load and suspended load. For points below the curve, the sediments are not transported. Although the experimental work and analysis were performed by Shields, Rouse (1939) first proposed the curve shown in Figure 9.

A problem with the Shields curve is that it is an implicit relation. The critical shear stress cannot be determined directly from the Shields diagram, although it must be known in order to determine particle motion. The critical shear stress must be determined through trial and error. Although engineers have used the Shields diagram widely as a criterion for incipient motion, discrepancies can be found in the literature. The shields relationship has been examined and modified by many researchers, including Vanoni (1975), Madsen and Grant (1975), Sleath (1984), Komar and Miller (1975).

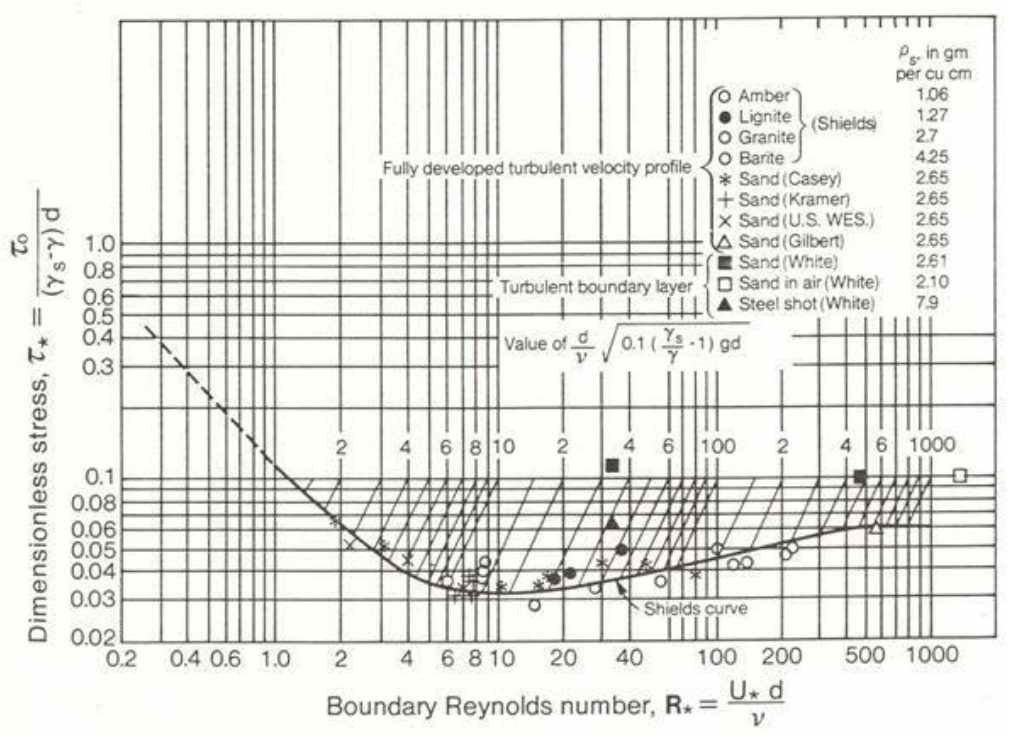

Figure 9. Shields curve for the initiation of motion.
(U.S. Army Corps of Engineers, 1995)

.

3 Marriott Reef Ball Breakwater Project

3.1 Erosion Issues

In 2002 the southern end of Seven Mile Beach had a serious erosion problem (Harris, 2003a). Figure 10 shows the severity of the erosion, with waves scouring underneath the seawall at the Marriott Hotel in October 2002. (Note that beaches in this area undergo profile changes throughout the year, due to seasonal changes in the wave characteristics. The extent of these changes is described in further detail in the following section). The major erosion issues in the Seven Mile Beach area were outlined by the Cayman Island Beach Review and Assessment Committee (BRAC, 2003) in a Strategic Beach Management Plan report as follows:

- Development on the beach ridge and dune system has removed the rapid self-healing capability from much of the length of the beach
- Beach ridge has been mined as a source of sand for local building and road construction
- Inappropriately sited structures, in particular seawalls, have been the root cause of almost all the development-induced problems on Seven Mile Beach
- The Seven Mile Beach system has been described as a "leaky beach" with potential for large losses of sand through gaps in the outer reef
- The Development and Planning Regulations have not adequately protected the beach over the years

- Recent weather patterns over the last 5 years have contributed to more erosion on the Southern section as a series of tropical storms have passed mostly to the South and West of the Cayman Islands

To understand the cause of this erosion in front of the Marriott, the following sections discuss these issues in further detail by examining the existing conditions, including seasonal cycles, littoral system, and recent storm activity.

Figure 10. View looking to the North at Marriott seawall in 10/02.
(Photo Courtesy of Lee Harris)

3.1.1 Environmental Conditions

Grand Cayman's small size and small tidal range means that the wind waves and large scale oceanic currents are the leading factors in water movement around the island (Blanchon and Jones, 1997). Figure 11 shows the typical direction of the currents, wind and storm directions, and location of the shelf-edge reef around Grand Cayman. The Caribbean Trade Winds blow from the northeast between 6-14 knots creating wind waves of significant height of 3.28 feet and a period of 6 seconds (Darbyshire *et al*., 1976), with Seven Mile Beach leeward of the winds and waves. The proximity of the shelf-edge reef contributes to the description of Grand Cayman as a "leaky beach" (BRAC, 2003). When sediment is transported out to sea, it is lost into a vertical drop-off known as the Cayman Wall, which begins about 600 feet offshore and drops to depths greater than 4000 feet.

Wave action is a major factor in the nearshore sand transport processes. Littoral transport occurs in the coastal areas of Grand Cayman (Darbyshire *et al*., 1976). Figure 12 is a schematic that shows the sand transport system of Seven Mile Beach. This transport system fluctuates with seasonal change and storm events, affecting the beach at the Marriott. During the wet season, May through November, high intensity storms and hurricanes move toward Grand Cayman from the east or south east along one of the two major hurricane paths that cross the Caribbean. These storms can cause waves that impact the Seven Mile Beach area from the southwest. When waves approach from the southwest, the beach sand along Seven Mile moves north, with some lost in deep water. The southern part of Seven Mile beach is highly susceptible to erosion from waves approaching from this direction because as one goes south from the Marriott there is only a short stretch of sand beach that is followed by a rocky shoreline and constructed groins. Harris (2003) states "… the reorientation of the shoreline and the rocky shoreline with no sediment source to the south prevent any potential natural transport of the sand from the south to the Marriott beaches."

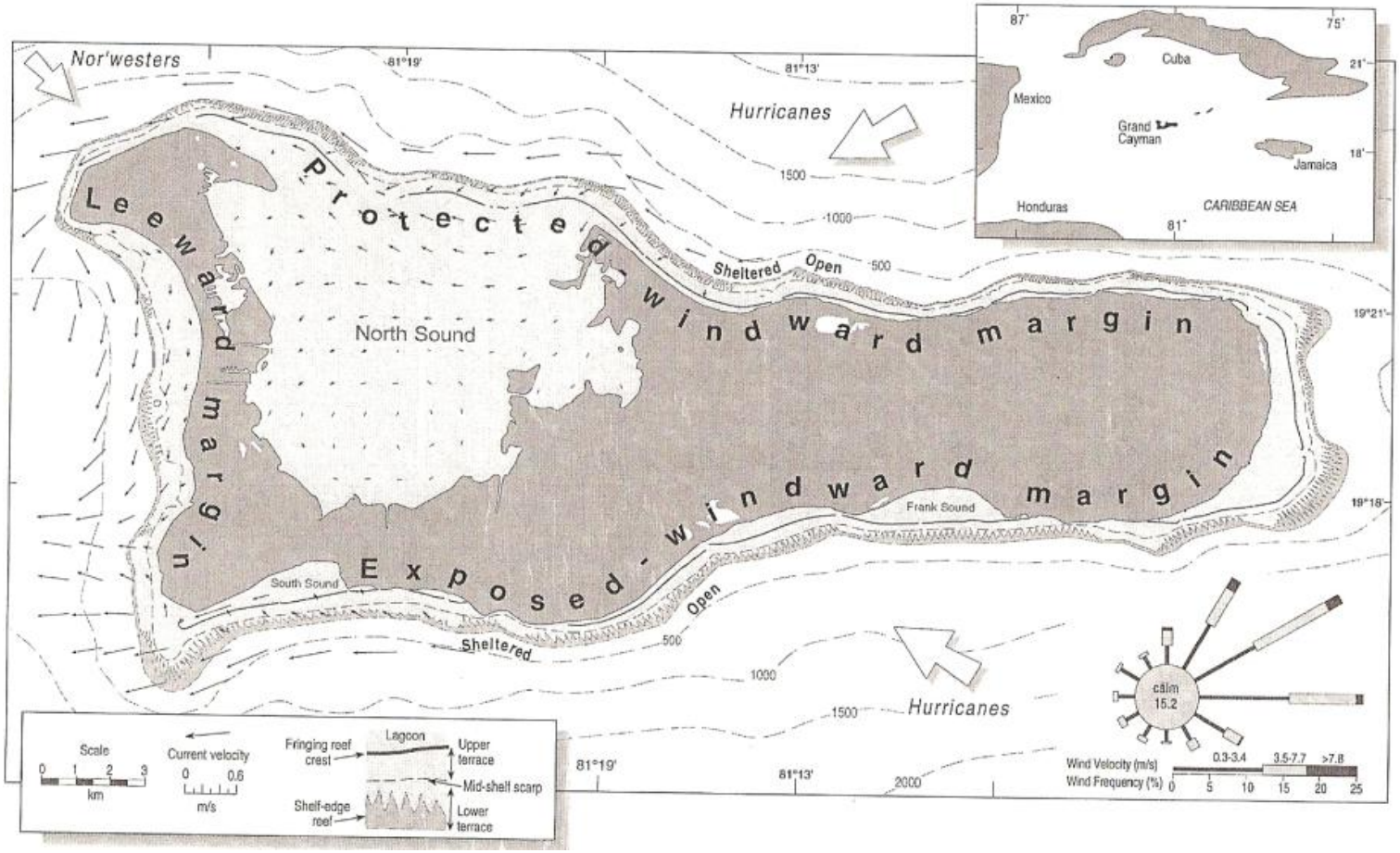

Figure 11. Grand Cayman's wind and storm directions, surface currents and details of shelf-edge reef. (Darbyshire *et al.*, 1976)

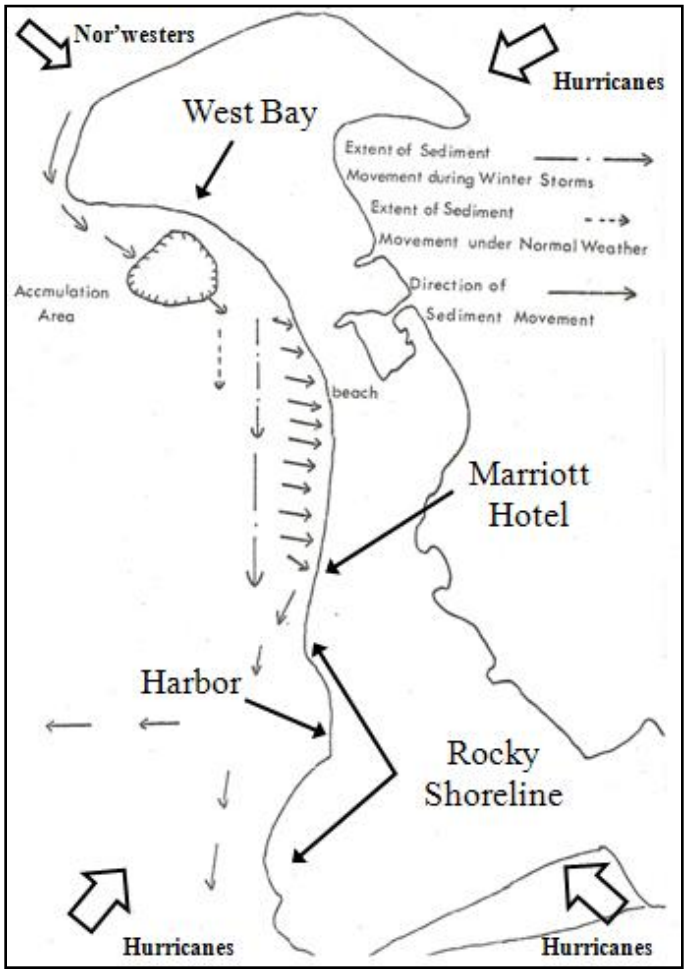

Figure 12. Typical Seven Mile Beach sand transport system. (Darbyshire *et al*., 1976)

During the dry season, December through April, the beach usually recovers naturally with sand from the north. This transport of material is induced by low intensity storms associated with continental cold fronts approaching Grand Cayman from the northwest (commonly known as nor'westers). This sand originates from strong currents around the north-western part of Grand Cayman. When the current slows, this material settles out and is dumped into northern Seven Mile Beach. Under normal conditions (non-storm), the average longshore current is only 0.1 ft/s, which is insufficient to move most sediments found in northern Seven Mile

Beach (Darbyshire *et al*., 1976). Only under winter storm conditions is the longshore current sufficient (about 0.23 ft/s) to move significant quantities of material (Darbyshire *et al*., 1976). During these low intensity "nor'westers," sediment is removed from this area and carried away in two main directions; south along Seven Mile Beach towards the Marriott and westwards out to sea. Although this process aids in the recovery of the Marriott Beach, more erosion and less recovery has been experienced in recent years.

Figure 13 shows this seasonal variation in terms of average beach width at the Marriott from 1999-2003. Storms and high wave action prevented the taking of measurements at times, which results in most of the gaps in the data (where beach widths are generally small). The width of the beach can fluctuate up to 50 feet seasonally due to the amount of storm activity within the year. In 2002, the shoreline retreated to the seawall, due to Tropical Storm Isidore in September and Hurricane Lili in October. The maximum beach width was only 45 feet in 2002, smaller than previous years. From the end of 2002 (after the Reef Balls were installed) to 2003, the beach accreted almost 60 feet in 3 months, the largest amount of accretion between seasons. In 2003, the beach continued to fluctuate seasonally, but maintained a positive average beach width.

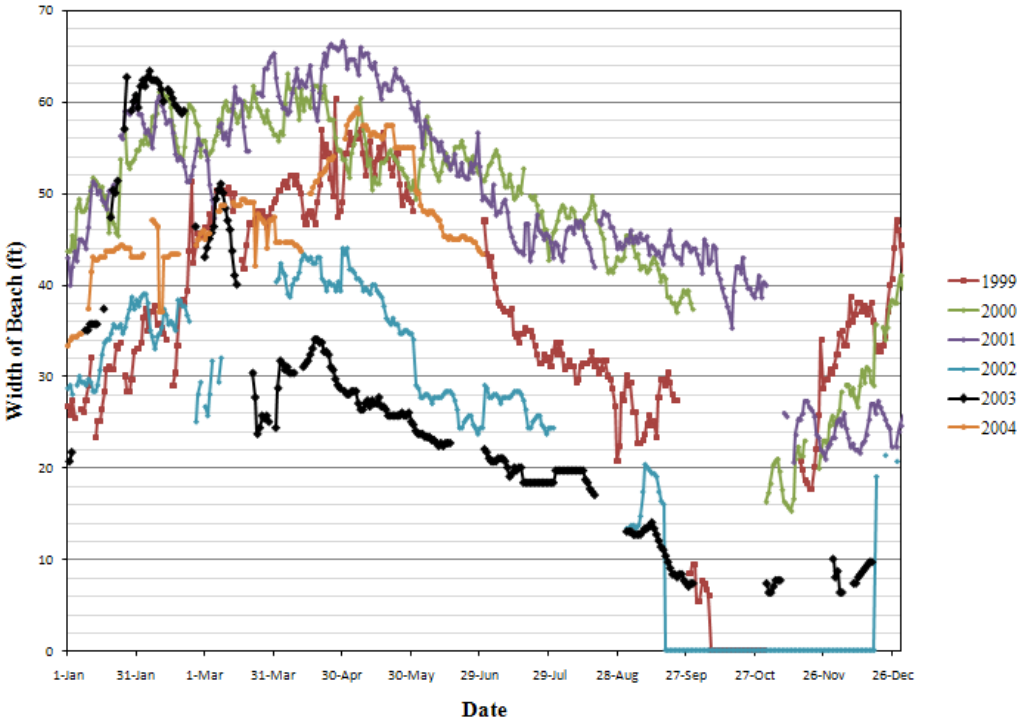

Figure 13. Seasonal beach width changes from 1999-2003.

As seen from Figures 14 and 15, the frequency of hurricanes and tropical storms approaching from the southwest has increased in recent years. Figure 14 shows the hurricane and tropical storm paths between 1971 and 1989. The majority of the storms approach Grand Cayman from the east or southeast. When storms and hurricanes approach more from the east, Seven Mile Beach is on the leeward side of the wind and waves. From 1990-2007, the storms switched from approaching from the East and Southeast to the Southeast and Southwest, as shown in Figure 15. The number of storms has also increased, producing strong winds and waves that affect Seven Mile Beach.

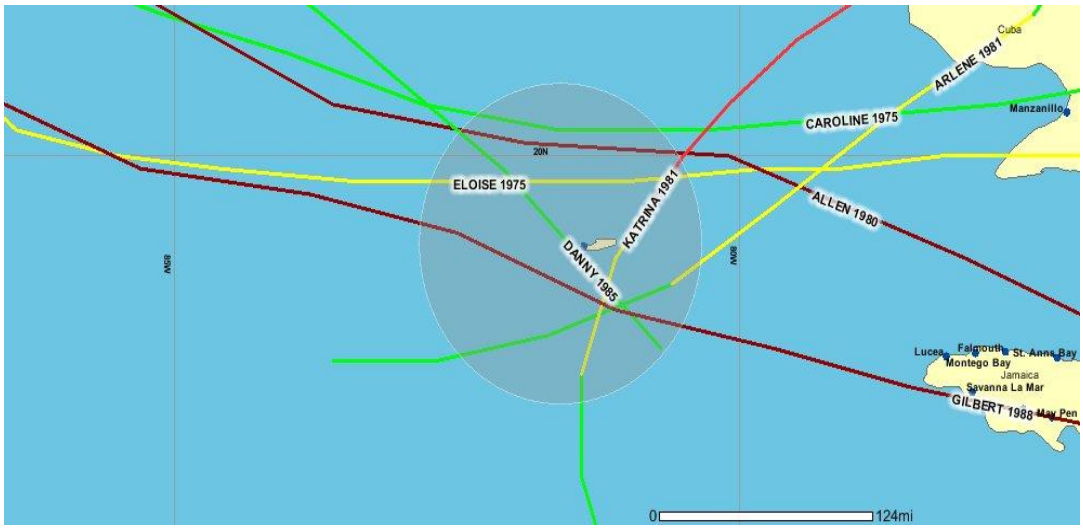

Figure 14. Hurricane and Tropical Storm paths near Grand Cayman. From 1971 to 1989. Note the majority of storms approaching Grand Cayman from the East. (NOAA Coastal Services, 2008)

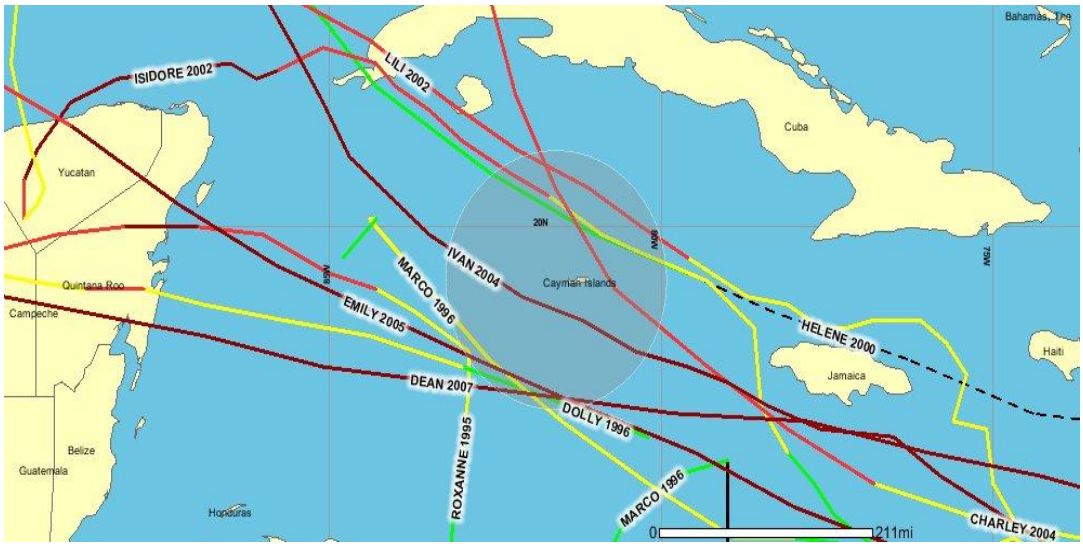

Figure 15. Hurricane and Tropical Storm paths near Grand Cayman. From 1990 to 2007. Note the majority of storms pass to the South and West of the Grand Cayman. (NOAA Coastal Services, 2008)

One storm of significant impact was Hurricane Ivan. On September 12, 2004, Category 5 Hurricane Ivan's center passed south of Grand Cayman. Strong winds (130 mph sustained, 149 mph gust), storm surge (8-10 ft), heavy rain (12.14 inches), flooding, heavy wave action, and coastal erosion had a detrimental effect on the island (Stewart, 2005). Young's (2004) study on the effects of Ivan on the island showed that the "variability in damage levels was entirely controlled by the presence or absence of shallow offshore coral reefs and the presence or absence of onshore winds during the storm." Fortunately, Seven Mile Beach did not receive continuous onshore winds, since the majority of the west coast has no shallow reef protection. The concern of severe wave damage to the exposed west coast of Grand Cayman during a storm track like Ivan could cause severe wave damage and surge flooding along Seven Mile Beach (Young, 2004). Appendix A contains a full list of storms with their corresponding category, dates, wind speed, and pressure.

3.1.2 Marriott Seawall

Seawalls are typically built on shorelines that are already eroding to protect upland structures. This is not the case for the Marriott Hotel seawall. When the Marriott Hotel was constructed in 1989, the pool and deck were constructed seaward of the hotel, but landward of a wide sand beach. When the beach eroded, the deck wall acted as a seawall when exposed to wave attack. Figure 16 shows that the beach was still very wide (approximately 100 feet) five years after the construction of the hotel. It was not until the early 2000's that the beach would recede enough to have waves directly impact the seawall to accelate or increase in the erosion. In a memo sent to the Marriott evaluating the effects of the existing seawall, Harris (2002) states that even if the seawall had not been constructed there would still be an erosion problem that would not be solved if the seawall was removed.

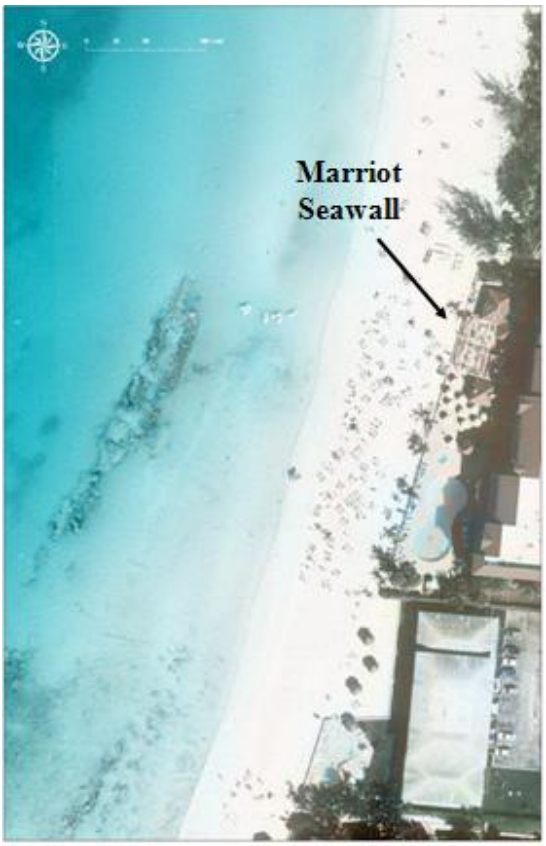

Figure 16. Aerial image from 1994 showing location of Marriott Seawall and width of beach in front of the seawall.

3.2 Marriott Reef Ball Breakwater Project

The Marriott Reef Ball Breakwater project was constructed to address the beach erosion at the Marriott Hotel. Reef Balls were designed to act as a submerged breakwater for shoreline protection, in addition to producing marine habitat, and providing hotel guests a chance to snorkel directly offshore. An aerial image shows the breakwater project in Figure 17. Visual observations of the study area are shown in Appendix C.

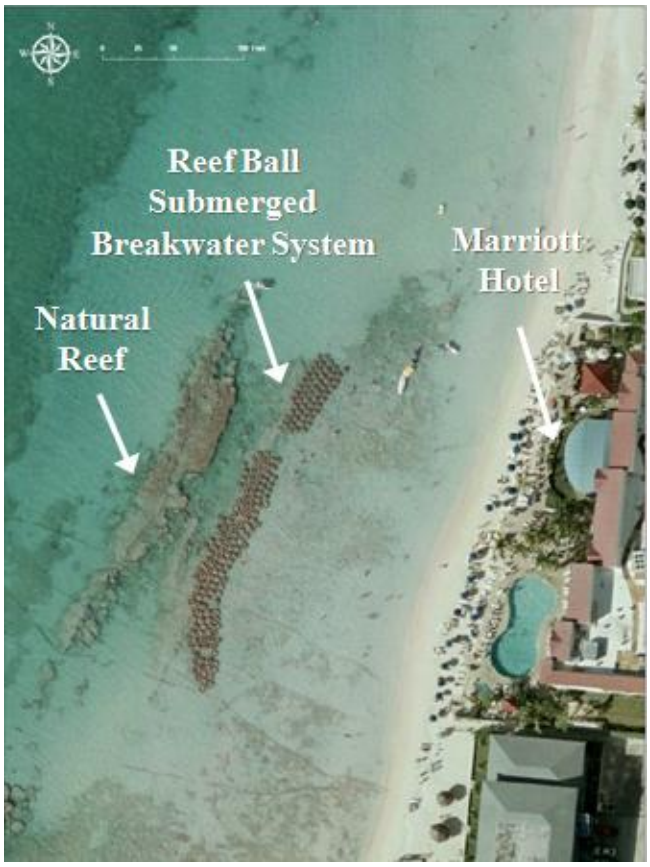

Figure 17. Aerial Image from 2004 showing the Marriott Reef Ball Submerged Breakwater Project.
(Photo Courtesy Tim Austin, Cayman Islands Department of Environment)

In 2002, approximately 200 Reef Ball units were deployed in front of the Marriott. The breakwater consisted of 5 rows of Reef Balls making it approximately 25 to 30 feet wide. The original design by Dr. Harris (2003) is illustrated in Figure 18. The heights of the Reef Ball units ranged from 3.7 to 4.5 feet, placed in water depths of 4.0 to 5.5 feet, making the top of the units just below the lowest normal water level (0.3 to 1.8 feet). In 2005, an additional 32 Reef Balls were added to the southern tip of the breakwater system. An opening in the breakwater was designed in front of the shallowest and widest part of the natural reef. The height of the natural reef in that area is 1.0 to 2.0 feet below the water level, which provides a similar level of protection as the Reef Ball breakwater. A

summary of design characteristics for the Marriott Reef Ball Breakwater is presented in Table 3, and a timeline for the project in Table 3. The bathymetry plot for the pre-breakwater survey conducted in August 2002 is illustrated in Figure 19. The plot depicts the location and depth of the natural reef.

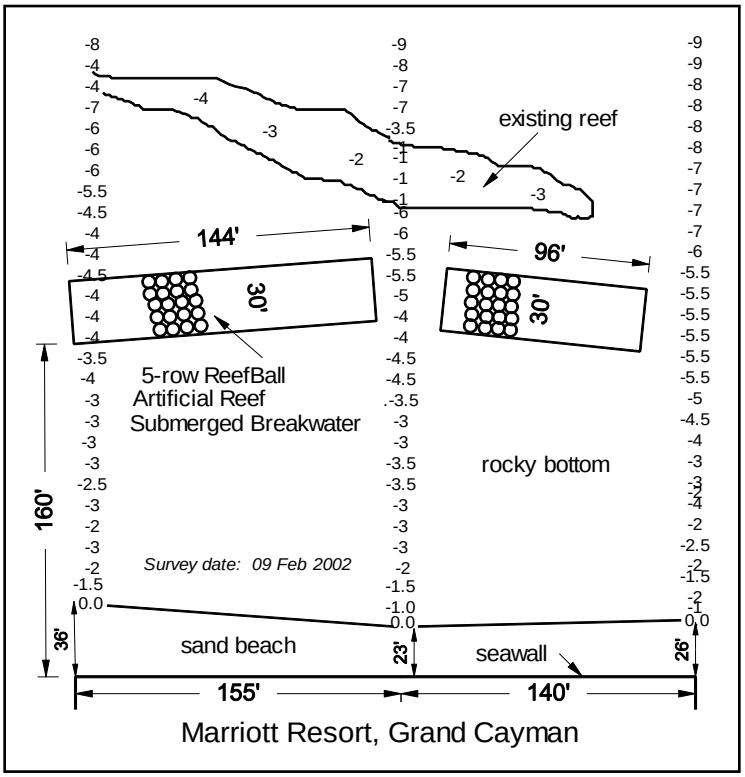

Figure 18. Initial design for Marriott Reef Ball Breakwater Project. (Harris, 2003a)

Table 3. Summary of design characteristic for Marriott Reef Ball Breakwater.

Freeboard	F (ft)	-0.7
Crest Width	B (ft)	25
Offshore distance of structure	S (ft)	4.8
Average water depth to toe of structure	d (ft)	4.1
Average structure height	h (ft)	0.16
Reef proportion	h/B	0.85
Depth of submergence	h/d	5.21
Relative width	B/d	-0.03
Relative structure height	F/B	-0.7

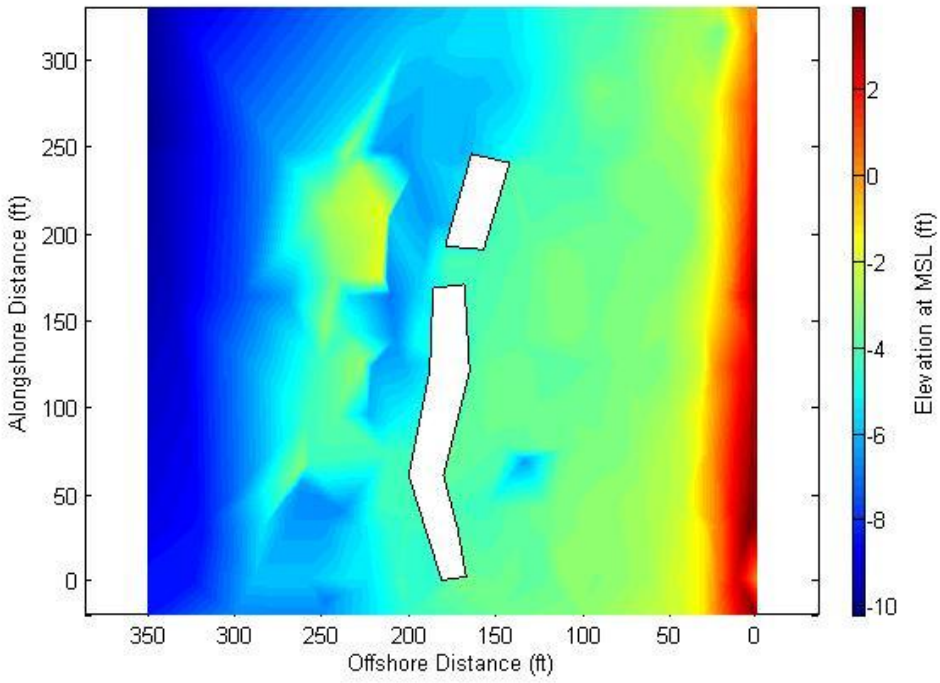

Figure 19. Bathymetry plot for in front of the Marriott Hotel in 08/02. The design for the breakwater system is outlined in black and white. Note the elevation of the natural reef between the gap in the breakwater.

Table 4. Timeline for Marriott Reef Ball Breakwater Project.

Prior to 2002		Aerial Images taken every 5 years starting in 1994
2002	August	Survey completed
	September	Tropical Storm Isidore
		Hurricane Lili (Cat 1)
	November	Survey completed
		Reef Balls Installed
2003	February	Survey completed
2004	April	Aerial Taken
	August	Hurricane Charley (Cat 1/2)
	September	Hurricane Ivan (Cat 4/5)
	November	Aerial Taken
2005	July	Hurricane Emily (Cat 4/5)
	November	Additional Reef Balls Installed
	December	Beach fill (6.0 cu yd/ft of material placed in front of the Marriott)
2006	N/A	Aerial Taken
2007	February	Survey completed
	August	Hurricane Dean (Cat 4)
2008	January	Survey completed
	June	Survey completed

The Reef Ball units chosen for this project were the Ultra Balls, weighing approximately 3000 lbs each (Harris, 2003a). To increase the stability and resistance to sliding, fiberglass rebar were driven through the units and into the bottom at an angle (Figure 20). For the Marriott Reef Ball Project, the sea bottom the Reef Balls were installed on predominantly barren rock with small areas of sand (Harris, 2003a).

Figure 20. Example of Anchored Reef Ball.
(Photo courtesy of Lee Harris)

4 Methodology

The shoreline analysis for the project area was accomplished using beach profile surveys, aerial images, and beach width data. Volumetric changes were calculated from the beach profile surveys. Wave transmission was calculated using the breakwater dimensions and a range of hydrodynamic conditions. The elevation and shoreline changes landward of the breakwater are presented in several formats to provide an overall assessment of the changes.

4.1 Data Sources

Initial monitoring and survey data were provided by Hadsphaltic International Ltd. under the direction of Dr. Lee Harris and then continued by Dr. Harris and the Reef Ball Foundation, Inc. Beach width data were taken by the Marriott Hotel staff, and aerial photographs were provided by Cayman Islands Department of Environment (DOE). Table 5 shows the types of data and corresponding years available for this area.

Table 5. Data available for Marriott Area from 1972 to 2008.

Type of Data	‘72	‘94	‘98	‘99	‘00	‘01	‘02	‘03	‘04	‘05	‘06	‘07	‘08
Beach Profile							x	x				x	x
Aerial Photos	x	x		x					x		x		
Beach Width			x	x	x	x	x	x	x	x			

4.2 Shoreline Changes

This study made use of all available data sources to produce a representation of the shoreline changes in front of the Marriott. Data sources fall into two categories: survey-based (beach profile and beach width data) and image-based (aerial photographs). The method of analysis and results obtained from each source category are discussed.

4.2.1 Survey-based

The series of beach profiles taken for this area provides important information to analyze the behavior of the beach. From the profile data, the performance of the breakwater can be studied through shoreline, volume, and cross-shore changes, and establishing an overall sand budget.

All surveys were referenced to the original pre-breakwater survey mean sea level (MSL) datum (0.6 ft), and corrected for tidal levels. The astronomical tide is characterized by a relatively low amplitude (about 1.0 feet) mixed diurnal and semi-diurnal system. The predicted tidal information for each survey date after February 2007 is included in Appendix B. The baseline for the profile lines was seawall, and the profile lines were extended seaward to and past the Reef Ball Breakwater. Shoreline position was based on interpolating values at the zero elevation contour. The four profile lines that were used are:

- Profile Line 1 (PL 1) – South end of breakwater
- Profile Line 2 (PL 2) – South end of Marriott seawall
- Profile Line 3 (PL 3) – Center of Marriott seawall
- Profile Line 4 (PL 4) – North end of Marriott Seawall

Figure 21 shows the location of the profile line. Sections South, Center, and North Structure correspond to the section between each PL 1 and PL 2, PL 2 and PL 3,

and PL 3 and 4, respectively. Table 6 shows the available profile data and their distance offshore.

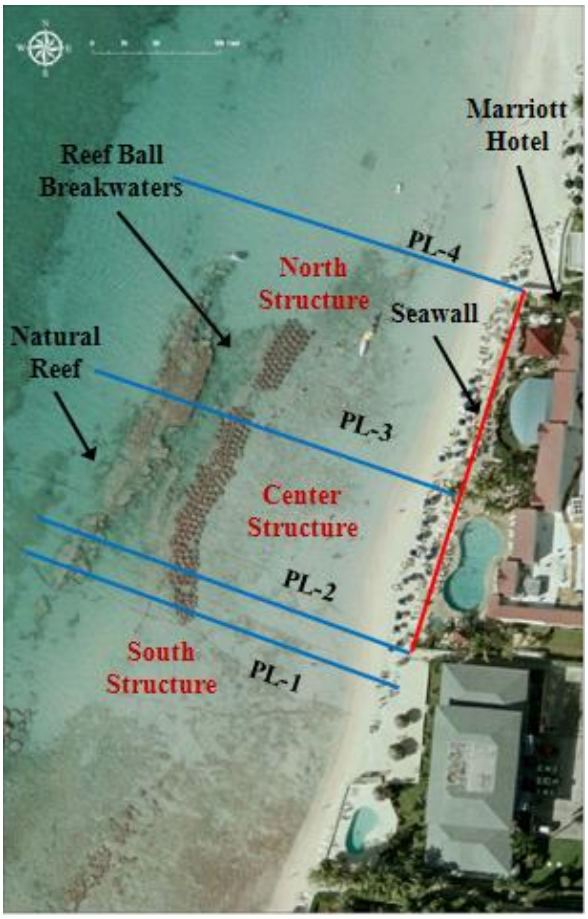

Figure 21. Location of beach profile survey lines (04/04).
Note: Photo predates southern breakwater extension.
(Photo Courtesy Tim Austin, Cayman Islands Department of Environment)

Table 6. Available Profile Data for the Marriott Hotel.

Date of Survey	Profiles Available	Distance Offshore (ft)	Elevation (ft)
8/29/02 (Pre- Reef Ball)	PL1- PL 4	200	-6.6
11/02 (As-Built Survey)	PL1- PL 4	180	-6.6
2/03/03 (3 Months After Installation)	PL1 - PL 3	210	-7
2/28/07	PL1- PL 4	180	-7
1/12/08	PL1- PL 4	220	-7
6/1/08	PL1- PL 4,	350	-10

Beach width measurements from 1998 to 2004 at the north, center, and south staircase of the seawall were supplied by the Marriott Hotel. Beach width data were measured out to the trough that forms immediately offshore of the shoreline position. Beach width measurements were used to analyze the relative beach width change and shoreline orientation before and after the breakwater were installed.

4.2.2 Aerial Photography

Aerial imagery was utilized to determine shoreline changes, which provide information between the beach profile survey dates. The geo-referenced, aerial images were loaded into ArcView3.2© using the ImageAnalyst © extension. Aerial images define the shoreline according to many different indicators discussed previously. Two issues for determining shoreline position for this study area are (1) the high clarity of water found offshore of Grand Cayman making determination of the waterline difficult, and (2) the unknown day and time of the photograph for adjustment of the tide level. Due to the quality of some of the aerial

images, the shoreline was defined by the most apparent shoreline feature. Aerial photos were available for the following dates,

- April 1972
- April 1994
- April 1999
- April 2004 (Pre-Hurricane Ivan (September 2004))
- November 2004 (Post-Hurricane Ivan (September 2004))
- 2006

April 1972 and 2006 aerials were not used in this study. April 1972 could not be geo-referenced, due to a lack of good reference points. The 2006 aerial was a mosaic of several months; therefore a specific time period could not be pin-pointed. Aerial photographs are presented in Appendix C.

4.3 Volumetric Changes

The area for volumetric change analysis corresponds to the available beach profile data. The cross-shore direction extends from the seawall to the breakwater, a distance of 170 feet. For volume changes, the average end area (AEA) method was used, represent as,

$$\Delta V = \sum_{i=1}^{n-1} \Delta x_i \ \frac{(A_i + A_{i-1})}{2}, \qquad (16)$$

where n is the number of profile lines, A_i and A_{i+1} are the areas for adjacent profile lines, and Δx is the distance between the profile lines. To account for the varying spacing between profile lines, volumetric changes are referred to as the change in volume per unit shoreline length using units of cubic yards per foot.

4.4 Wave Transmission

Wave transmission was calculated using the four methods described in section 2.1.3 and compared. The breakwater design parameters required for the wave transmission equations are shown in Appendix E. Wavelength was calculated using the linear dispersion equation, represent by,

$$\sigma^2 = gk\ tanh(kd), \qquad (17)$$

where $\sigma = (2\pi)/T$, $k = (2\pi)/L$, and d is the water depth. Since wave data were not available, the transmission coefficient, K_t, was calculated for wave periods ranging from 4-10 seconds and wave heights ranging from 1-10 feet. This range is typical for the west side of Seven Mile Beach area (Darbyshire *et al*., 1976). To determine the largest wave height approaching the breakwater before breakin, the spilling breaker assumption was used. The spilling breaker assumes that the wave height within the surf zone is a linear function of the local water depth (ignoring bottom slope). To determine the maximum wave height the following equation is used:

$$H = \kappa h \qquad (18)$$

where κ, the breaker index, is on the order of 0.8 (Dean and Dalrymple, 2002). Using this assumption, the largest wave height approaching the breakwater before breaking is 3.84 feet. To include wave transmission during storms storm surge was calculated for wave heights greater than 3.84 feet.

4.5 Sediment Transport

Using the calculated wave transmission, the transmitted wave height and resulting horizontal water particle velocity were determined. This information, in addition to the sediment characteristics, was used to determine if the sediments leeward of the breakwater will be transported according to the Shields Diagram (Figure 9).

The horizontal water particle velocity for the transmitted wave height was determined using the following linear wave theory equation:

$$U = \frac{H}{2}\frac{gT}{L}\frac{\cosh\left(2\pi\left(\frac{z+d}{L}\right)\right)}{\cosh\left(\frac{2\pi d}{L}\right)}\cos\theta \qquad (19)$$

where z is the depth at which the water particle velocity is calculated, and cosθ varies from +1.0 to -1.0, with the maximum value taken as ±1.0.

Sediment characteristics for the sand found in front of the Marriott Hotel was done using sieve analysis. Figure 22 shows the grain size distribution curve for a log-normal grain size distribution, with the median diameter d_{50}= 0.43 mm (0.0014 feet). The sand sample report is in Appendix D.

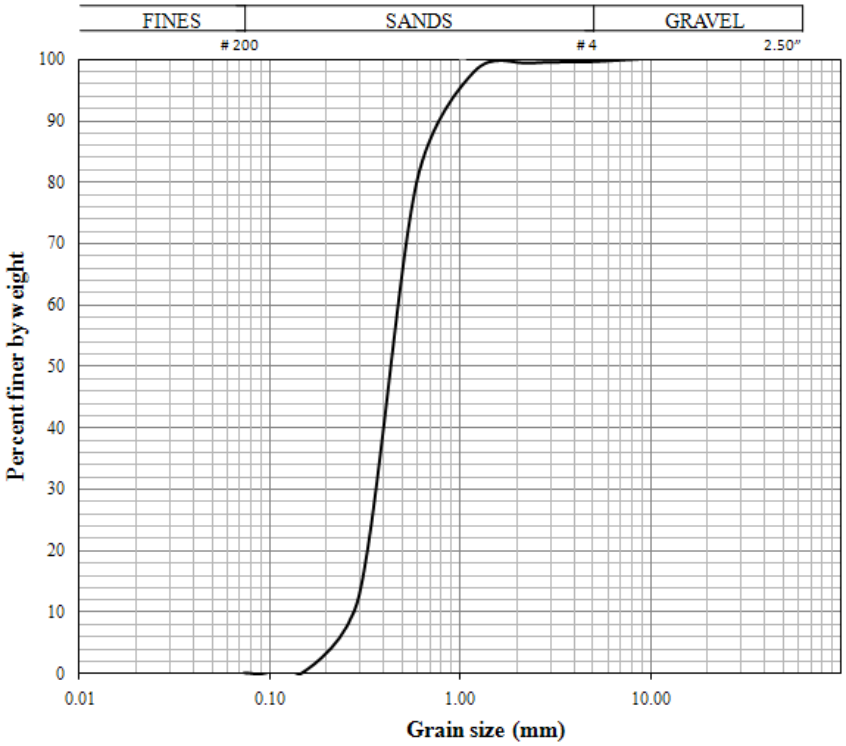

Figure 22. Grain size distribution curve.

From the Shields curve it was possible to determine the wave parameters to initiate sediment motion. To do this the bottom shear stress was calculated and then the wave height that produces the appropriate velocity was determined. The boundary shear stress responsible for initiation of sediment transport was determined through trial and error by plotting the resulting shields shear stress against the grain Reynolds number. When the point was above the curve, the sediments theoretically are transported. The variables used to find the grain Reynolds number and Shields parameter are shown in Table 7 and are used in Equations 14 and 15 to determine τ_*, and R_*.

Table 7. Variables used to determine the critical shear stress.

Variable		Symbol	Units
Grain density	165.43	ρ_s	lb/ft^3
Fluid density	64.3	ρ_f	lb/ft^3
Gravitational acceleration	32.2	g	ft/s^2
Grain diameter	0.0014	d_s	ft
Dynamic viscosity	8.10E-04	μ	lb/ft s
Kinematic viscosity:	1.26E-05	ν	ft^2/s^2
Shear velocity	0.05	u_*	ft/s

The velocity required to move the sediment can be determined by solving the following equation for bed shear stress for the flow velocity, *U*:

$$\tau_0 = \frac{1}{8}\rho_f f U^2 \qquad (20)$$

where f is the Darcy-Weisbach friction coefficient (typically 0.025-0.03 for sand) (U. S. Army Corps of Engineers, 2006b).

5 Project Performance

The Marriott Reef Ball Breakwater was installed in 2002 to control the Marriot's beach erosion problem. The performance of the Reef Ball breakwater is presented through shoreline, volumetric, cross-shore, and wave transmission analysis.

5.1 Shoreline Changes

5.1.1 Plan View

Pre-breakwater installation shorelines are displayed in Figure 23. In 1994 the beach width was the greatest at 90 feet. The shoreline continued to retreat until 8 years later, the shoreline reached the seawall. Post-breakwater installation shorelines are displayed in Figure 24. In 11/02, the beach width was zero feet. Three-months after installation, the shoreline accreted an average of 50 feet. The narrowest beach width was in 11/04 following Hurricane Ivan. In 02/07, four years after the project, the middle of the beach reached 82 feet wide, almost as wide as the 1994 beach. Between an average of 50 and 70 feet of beach width occurs during the winter/spring, decreasing to 10-20 feet in the fall following tropical storm events.

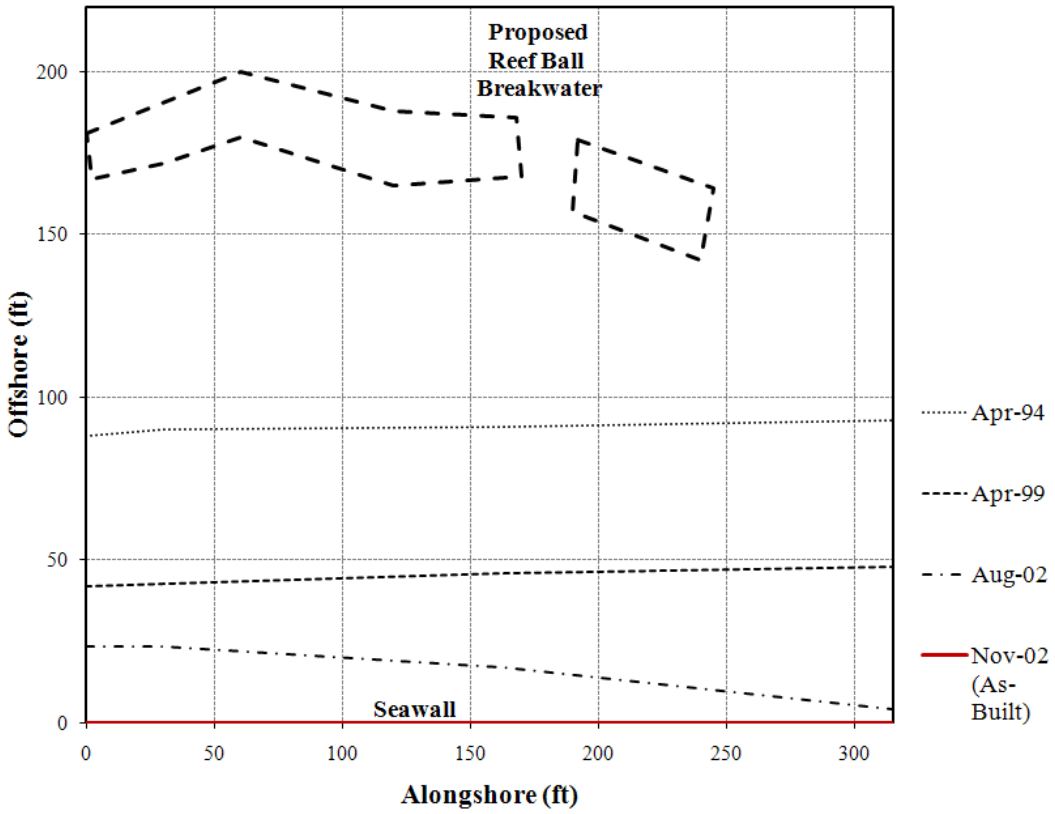

Figure 23. Location of shoreline from 04/94 to 11/02 (pre- breakwater installation).

\

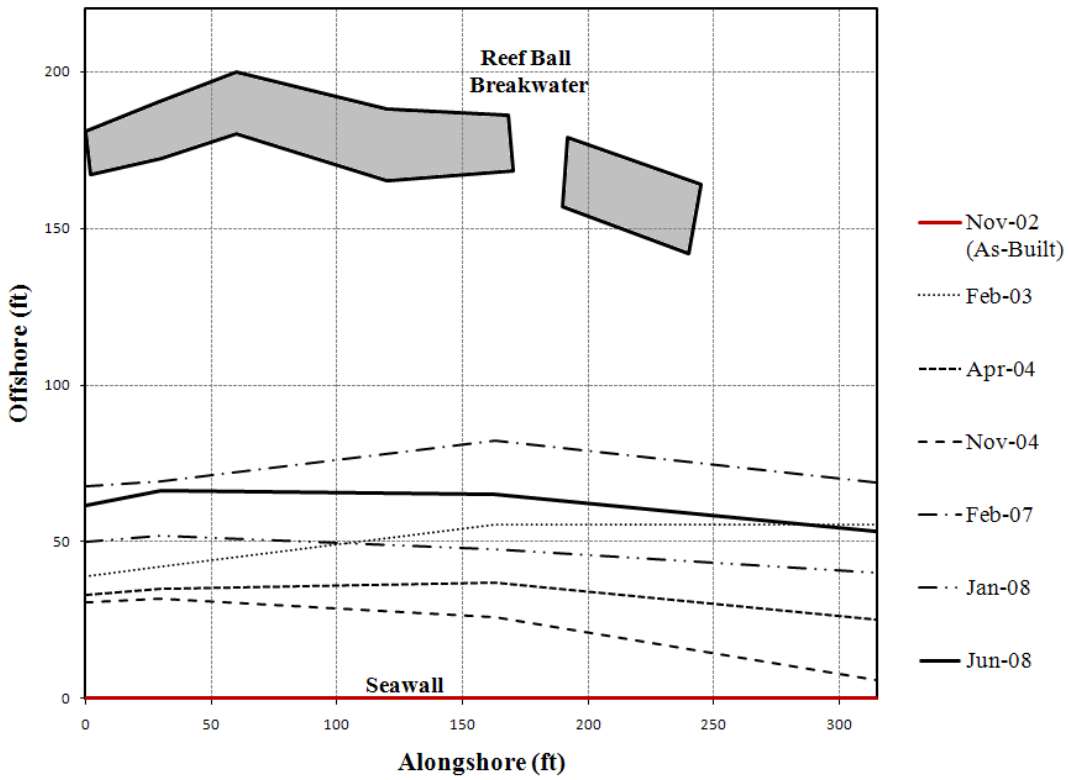

Figure 24. Location of shoreline from 11/02 to 06/08 (post-breakwater installation).

Table 8 presents the summary of mean shoreline changes and the annual average shoreline changes in feet per year (shoreline change was divided by the time period in a year to annualize the shoreline change). Seasonal fluctuations are also seen in Table 8 and Figure 24. From fall to spring, the rate of change is always positive, and from spring to fall, the rate of change is negative.

Table 8. Average shoreline position and rate of change.

Survey Date	Mean Shoreline Position (ft)	Time Period	Mean change (ft)	Annualized Mean Change (ft/yr)
04/94[1]	90.50			
04/99[1]	44.75	04/94-04/99	-45.75	-9.15
08/02[2]	16.82	04/99-08/02	-27.93	-8.38
11/02[2]	0.00	08/02-11/02	-16.82	-67.29
02/03[2]	47.91	11/02-02/03	47.91	191.65*
04/04[1]	32.50	02/03-04/04	-15.41	-13.21
11/04[1]	23.75	04/04-11/04	-8.75	-15.00
02/07[2]	72.02	11/04-02/07	48.27	21.45
01/08[2]	47.30	02/07-01/08	-24.72	-26.97
06/08[2]	61.60	01/08-06/08	14.30	34.31

Notes: (1) From aerial photographs
(2) From survey data
* Post-breakwater installation survey

Table 9 presents the average annual shoreline change, for pre and post breakwater construction. Before the breakwater was installed all profile lines eroded consistently around -10.5 ft/yr. After installation of the breakwater, the shoreline began to accrete at a mean rate of +11.0 ft/yr. Profile Line 4 accreted the slowest (+11.0 ft/yr), and PL 2 accreted the fastest (+ 11.6 ft/yr).

Table 9. Average annual shoreline changes.

	Average annual change (ft/yr)				
	PL 1	PL 2	PL 3	PL 4	Mean
04/94-11/02 (Pre-BW)	-10.25	-10.49	-10.60	-10.83	-10.54
11/02-06/08 (Post-BW)	11.05	11.87	11.63	9.52	11.02

5.1.2 Time Series

Figure 25 shows the total cumulative shoreline change from 1994 to 2008. Since completion of the breakwater project, the shoreline change from 1994 is decreasing, which shows the shoreline width is increasing to the 1994 shoreline width. Prior to construction of the breakwaters, the shoreline retreated an average of -90 feet to the seawall. After the breakwater placement in 2002, the beach continued to show seasonal fluctuations, but maintained shoreline positions seaward of the seawall. It is important to note that PL 4 (northern end of the seawall) does not increase in beach width as much as the other 3 profile lines. Conversely, PL 2 shows the greatest increase. The largest retreat on the northern end of the beach was in 11/04, 2 months after Hurricane Ivan in September.

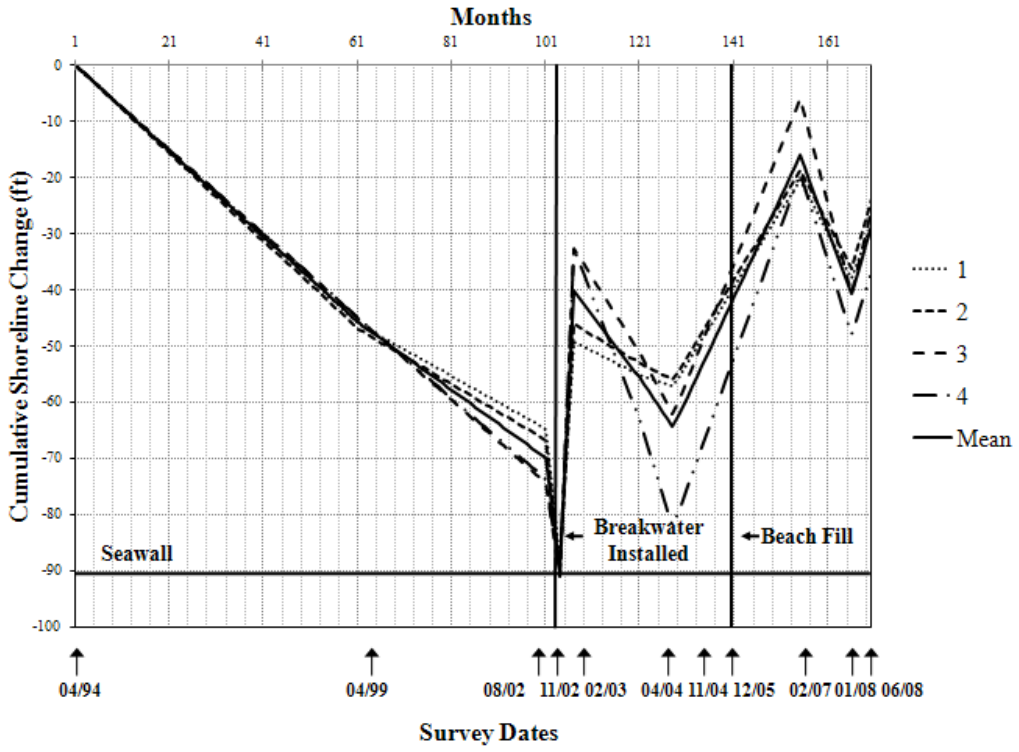

Figure 25. Cumulative shoreline change (from 04/94 to 06/08).

5.2 Beach Profile Changes

Construction of the Reef Ball breakwater concluded in November 2002 with 200 units being installed. Installation of the southern extension (32 additional units) was completed between September and November of 2005, and a beach fill of 6.0 cy/ft in December 2005 by the Cayman Islands Government. The results in this section are presented for the following three periods:

- Changes after initial installation but before the extension (11/02 to 02/03)
- Changes after installation of the extension and beach fill (02/03 to 02/07)
- Overall change since installation (11/02 to 06/08)

Figures 26, 27, 28, and 29 illustrate the evolution of the beach profiles for PL 1, PL 2, PL 3, PL 4, respectively, since 08/02. The dashed lines represent pre-breakwater and the solid lines represent post-breakwater construction.

In 11/02, the as-built survey for construction, the highest elevation was below mean sea level and water was at and under the seawall. Three months post-construction, there was a significant increase in elevation (+3 to +5 feet) due to accretion in PL 1-3. The center of the breakwater had a gentler slope, with the widest beach width (55 feet), but the lowest elevation (2.5 feet), than to the south of the breakwater.

Between 2003 and 2007, the largest elevation and berm width increase on the shoreface is seen in all profile lines. Elevations at the seawall increased 1 to 2 feet. The berm height (+2 to +3 feet) and width (+20 to +30 feet) also increased significantly. From 2007 to 2008, the profiles steepened back to the before extension and beach fill period, presumably reaching equilibrium. Two and a half years after the beach fill (06/08), the beach width and height is still greater than two years before the fill in 02/03.

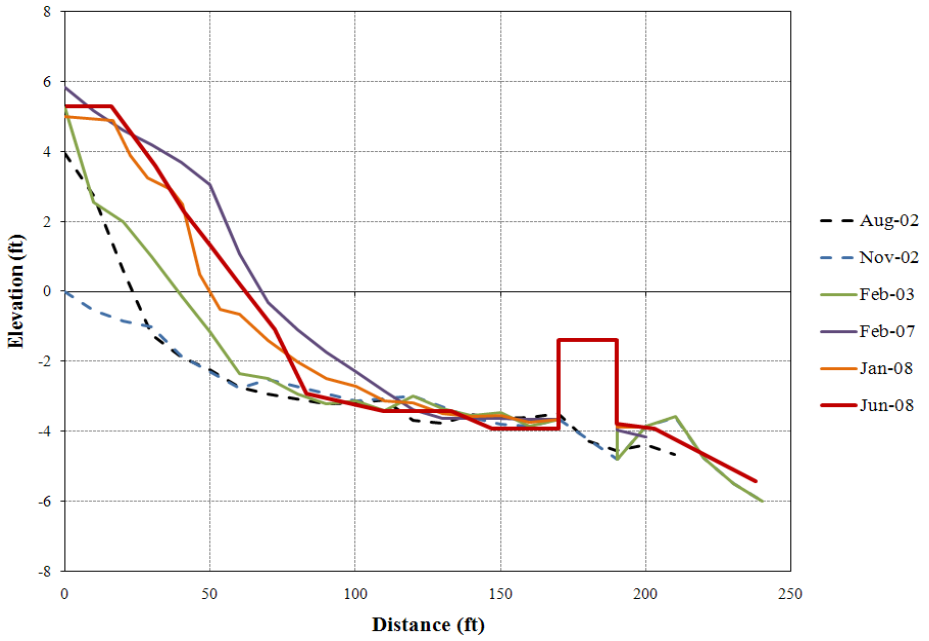

Figure 26. Cross-shore positions for PL 1 (South end of breakwater). The dashed lines represent pre-breakwater and the solid lines represent post-breakwater construction.

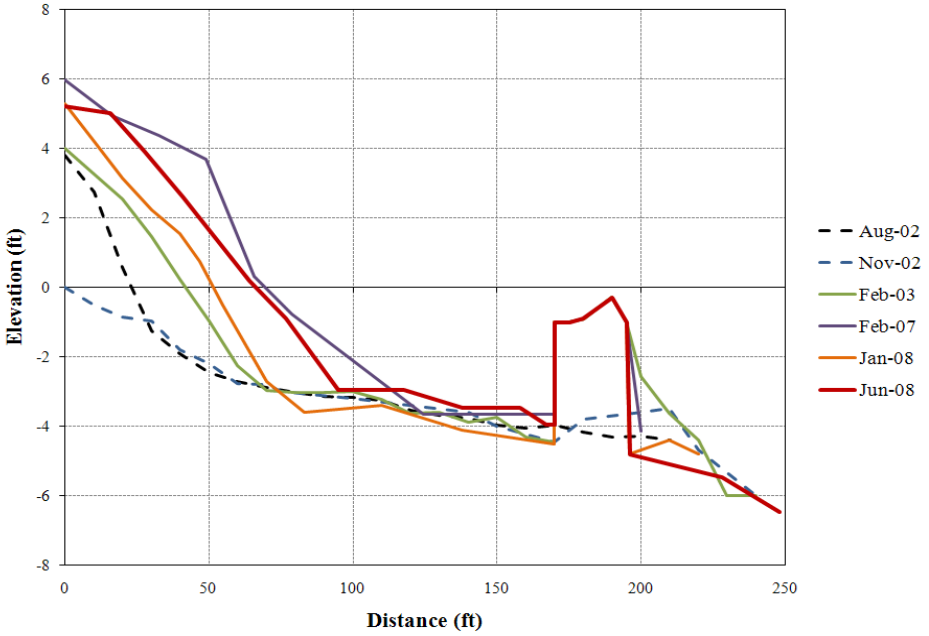

Figure 27. Cross-shore positions for PL 2 (South end of seawall). The dashed lines represent pre-breakwater and the solid lines represent post-breakwater construction.

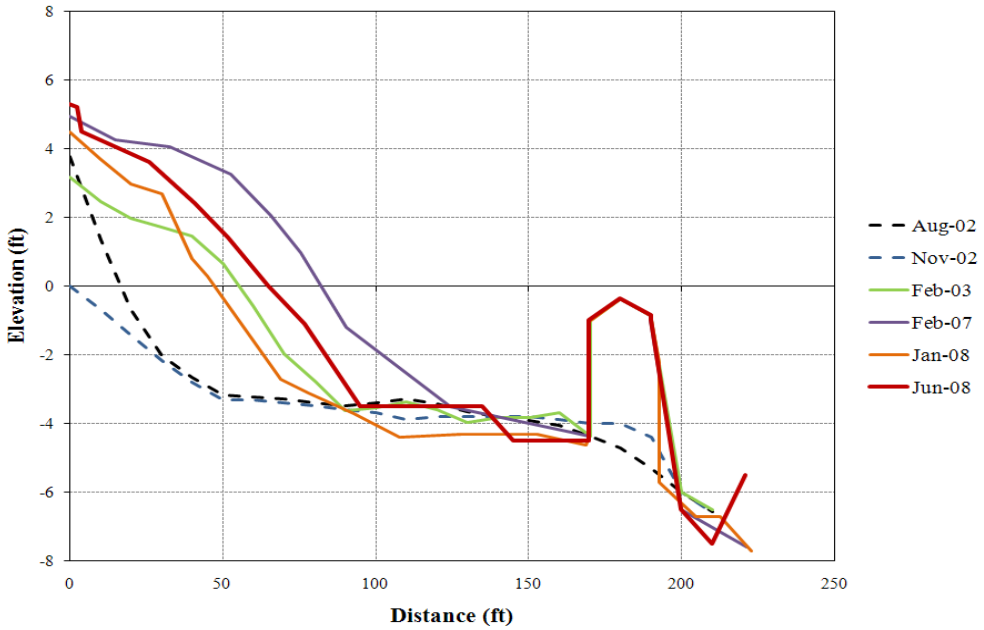

Figure 28. Cross-shore positions for PL 3 (Center of seawall). The dashed lines represent pre-breakwater and the solid lines represent post-breakwater construction.

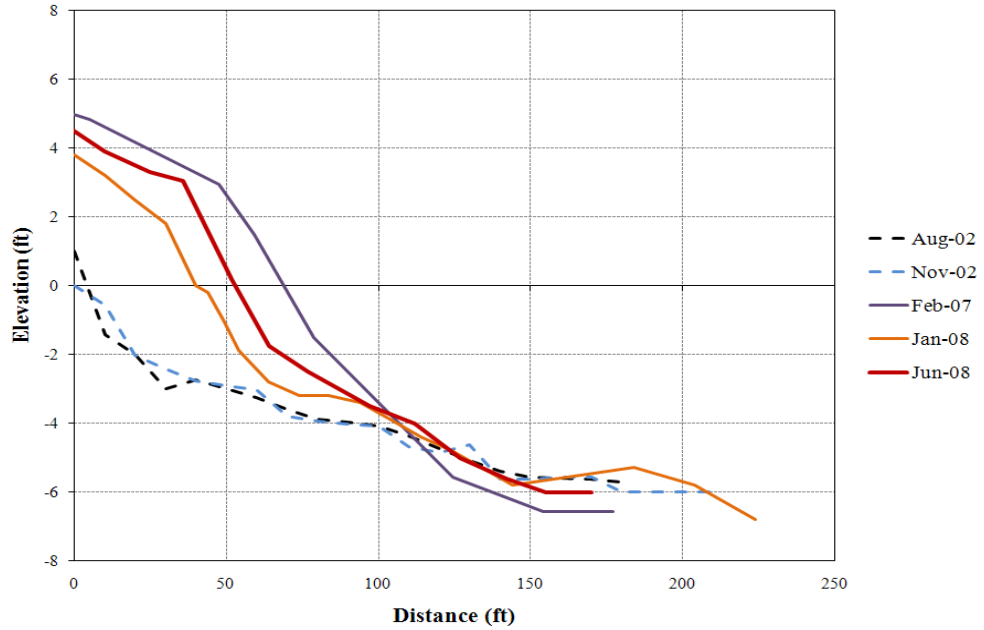

Figure 29. Cross-shore positions for PL 4 (North end of seawall). The dashed lines represent pre-breakwater and the solid lines represent post-breakwater construction. Note missing profile line for Feb. 2003.

5.3 Volumetric Changes

Volume changes represent the quantity of sand remaining within the project area. Due to the different distances between profiles, results were normalized to volume per linear foot (cy/ft) for the net and cumulative volume change rates. Volume changes extend from the toe of the seawall out to the breakwater (water depths around -4.0 to -5.0 feet), and are presented for all profile lines broken into three sections:

- South Structure (PL 1 to PL 2)
- Center Structure (PL 2 to PL 3)
- North Structure (PL 3 to PL 4).

The volume changes are shown for each survey period in Table 10. Note that PL 4 was not measured by the surveyors in 02/03. The value for that section was estimated by applying the percentage of the South and Center sections from 11/02 to 02/03 and 2/03 to 02/07 to the total from 11/02 to 02/07 (approximately 40% from 11/02 to 02/03 and 60% from 02/03 to 02/07) to the North section in 02/03. The total cumulative volume change was +3760 cubic yards from 08/02 to 06/08 (Post-breakwater).

Table 11 shows the volume changes per unit width of beach for each survey period to account for the different distances between profile lines. The largest increase of volume per unit beach length is seen between 02/03 and 02/07, an average 11.4 cubic yard per foot. Between those time periods (fall of 2005), there was a 6.0 cy/ft beach fill and an extension of the breakwater to the south. From 02/07 to 01/08 the volume decreased in all sections, with the greatest loss in front of the Center section. Conversely, from 01/08 all sections began to increase, with the largest increase in front of the Center section. This section shows the most fluctuation. The South section shows the least amount of fluctuation. Table 12 and Figure 30 show the annualized volume change to account for the different lengths

between survey dates. The annualized volume change of the beach fill between 02/03 and 02/07 is 1.5 cy/ft/yr.

Table 10. Volume changes for each survey period.

	Volume Changes (cy)			
	South	Center	North	Total
08/02 to 11/02	-61.42	-320.83	-131.59	-513.84
11/02 to 02/03	157.86	1014.99	1092.54	2265.39
02/03 to 02/07	333.53	1534.01	1638.81	3506.35
02/07 to 01/08	-225.36	-1536.22	-1490.25	-3251.83
01/08 to 06/08	139.34	868.47	746.26	1754.07
Total	343.96	1560.41	1855.78	3760.15

Table 11. Volume changes per unit width of beach for each survey period.

Survey Dates	Volume Changes per unit width (cy/ft)			
	South	Center	North	Average
08/02 to 11/02	-2.05	-2.41	-0.87	-1.78
11/02 to 02/03	5.26	7.63	7.19	6.69
02/03 to 02/07	11.12	11.53	10.78	11.14
02/07 to 01/08	-7.51	-11.55	-9.80	-9.62
01/08 to 06/08	4.64	6.53	4.91	5.36
Total	11.47	11.73	12.21	11.80

Table 12. Annualized volume changes per unit width of beach for each survey period.

Survey Dates	Annualized Volume Changes per unit width (cy/ft/yr)		
	South	Center	North
08/02 to 11/02	-8.19	-9.65	-3.46
11/02 to 02/03	21.05	30.53	28.75
02/03 to 02/07	2.78	2.88	2.70
02/07 to 01/08	-8.19	-12.60	-10.70
01/08 to 06/08	11.15	15.67	11.78

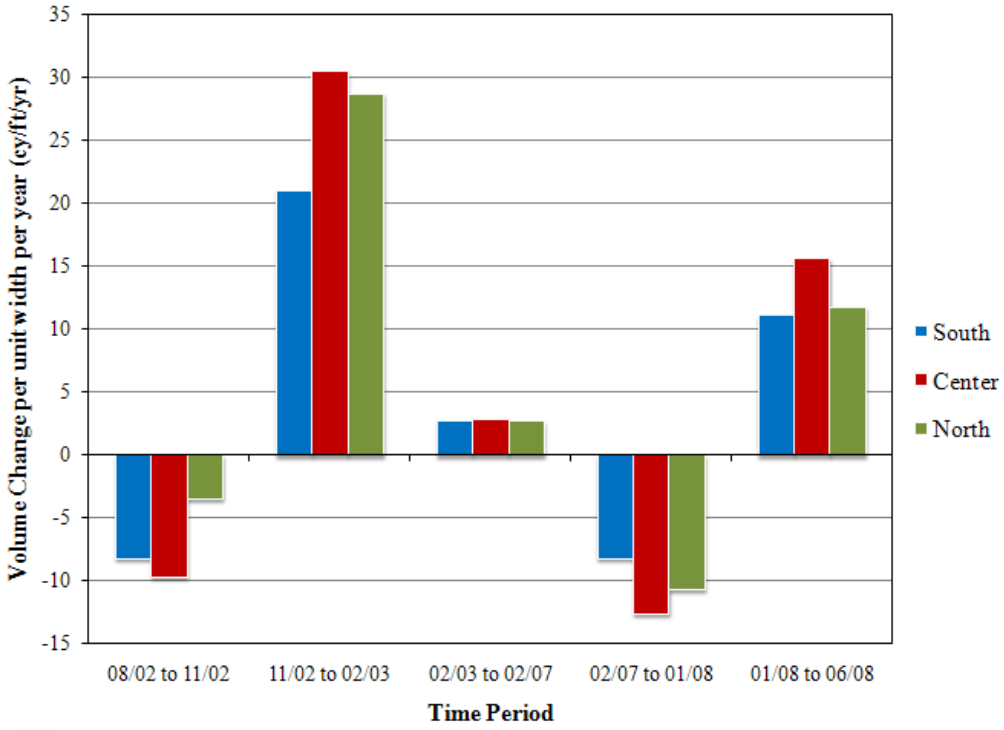

Figure 30. Annualized volume changes between surveys.

Table 13 provides cumulative volumetric profile changes per unit with from 11/02 (As-built) to each of the survey dates and Figure 31 illustrates them graphically. To account for the variable time periods, a time series plot of the cumulative volume change per unit width from 11/02 is shown in Figure 33. Accretion was seen in all survey periods post-construction. The largest volume increase (+35.5 cy/ft) was seen after the beach fill and breakwater extension at the end of 2005 from 11/02 to 02/07. The largest volume increase in between sections was seen in front of the Center Breakwater section in all survey periods except for 01/08. The volume in the northern section of the breakwater was larger than the south in 02/07, but smaller in 01/08 and 06/08. From 11/02 to 06/08 the total volume increase was +27.6 cy/ft, a -7.8 cy/ft decrease from 02/07.

Table 13. Cumulative volume changes per unit width from 11/02 (As-Built).

11/02	Volume changes per unit width (cy/ft)			
to	02/03	02/07	01/08	06/08
South	5.26	16.38	8.87	13.51
Center	7.63	19.17	7.61	14.14
North	7.19	17.10	7.30	12.21
Totals	12.89	35.55	16.48	27.66

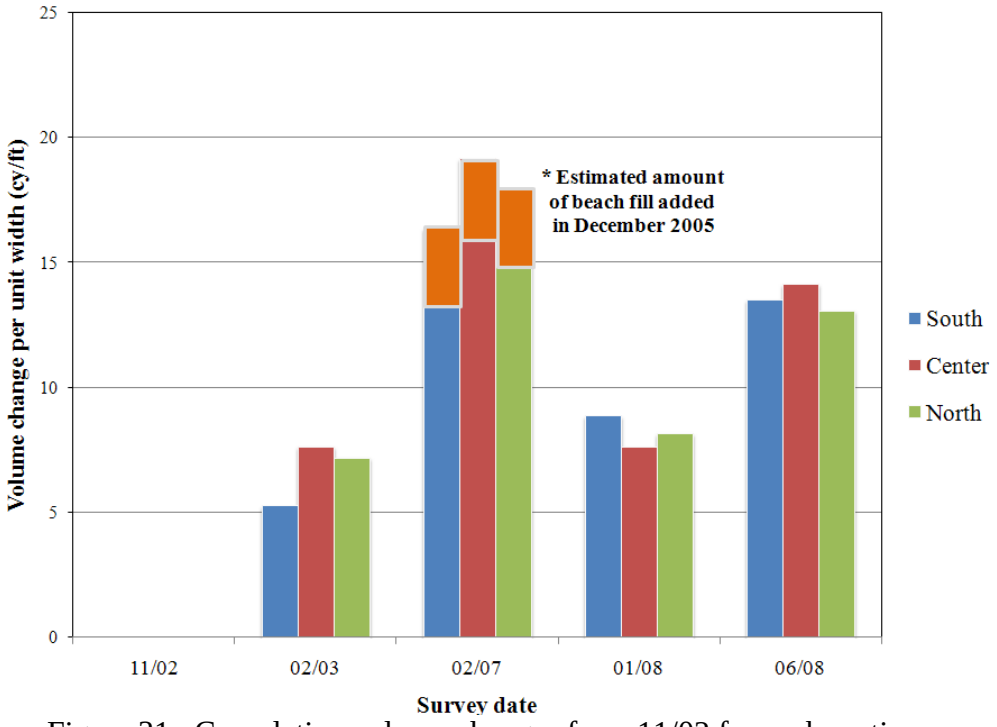

Figure 31. Cumulative volume changes from 11/02 for each section.

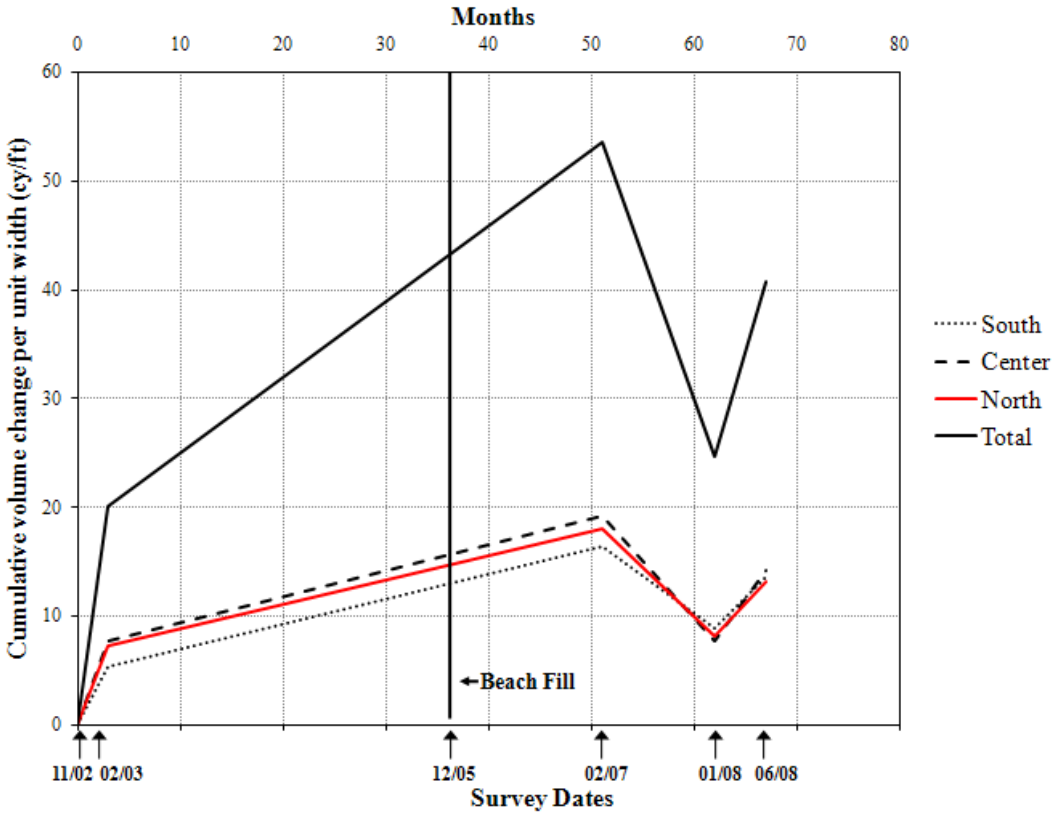

Figure 32. Time series cumulative volume changes per unit width from 11/02.

5.4 Wave Transmission

The transmission coefficient is used to measure the effectiveness of a breakwater in terms of wave attenuation. Figures 33 and 34 show the predicted transmission coefficient, K_t, for various wave heights at a wave period of 4 and 10 seconds, respectively. The transmission coefficients for wave periods between the 4 and 10 seconds are shown in Appendix E. For instances with no storm surge, the transmission coefficient continues to decrease as the wave height increases. When there is storm surge and the water depth and wave height increase, the transmission coefficient continues to increase. The Friebel and Harris method show the least

amount of transmission over the breakwater, with reduction of wave heights by at least 60% for instances with no storm surge.

The varying results between methods are due to limitations in the methods. Friebel and Harris' equation was developed from data collected in 2D wave tanks and did not allow for refraction, only transmission passing directly over the crest of the breakwater. In a 3D case, refraction allows more wave energy in the lee of the structure. Ahrens and Seabrook and Hall's methods resulted from wave tank physical model tests using rubble mound armor stone, not Reef Ball units. Also, Ahrens' method takes into account varying crest height. Although Armono and Hall used hollow hemispherical shaped artificial reefs, including Reef Ball units, all of the parameters of the breakwater system in this study did not fall into the range of recommended design parameters.

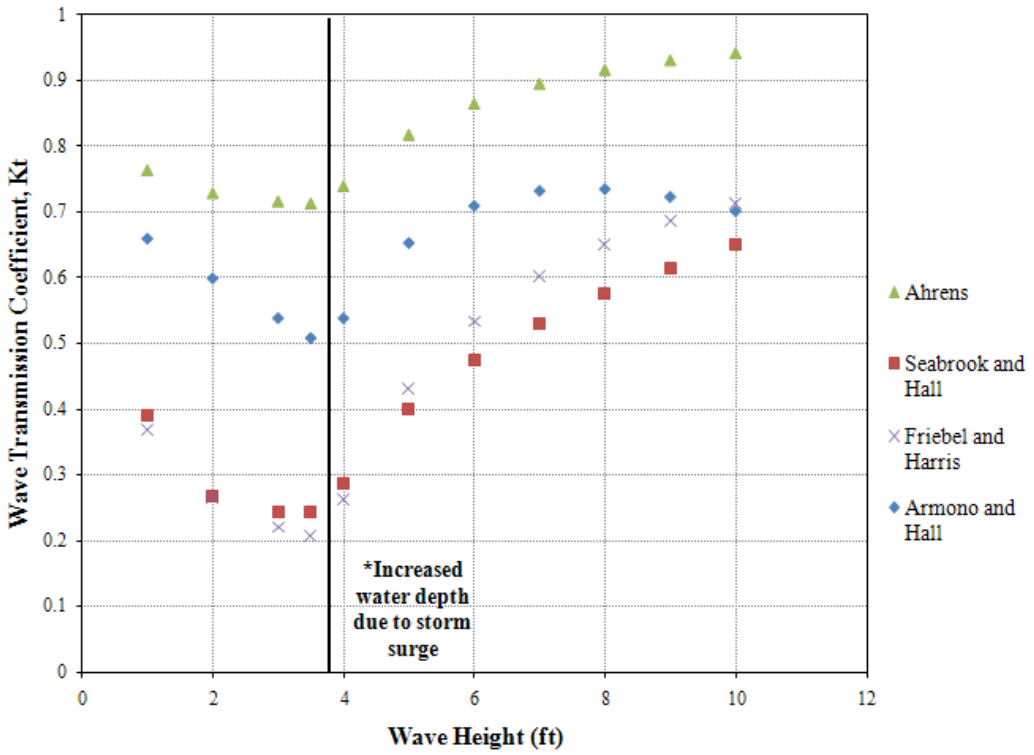

Figure 33. Wave transmission coefficient for a wave period of 4 seconds.

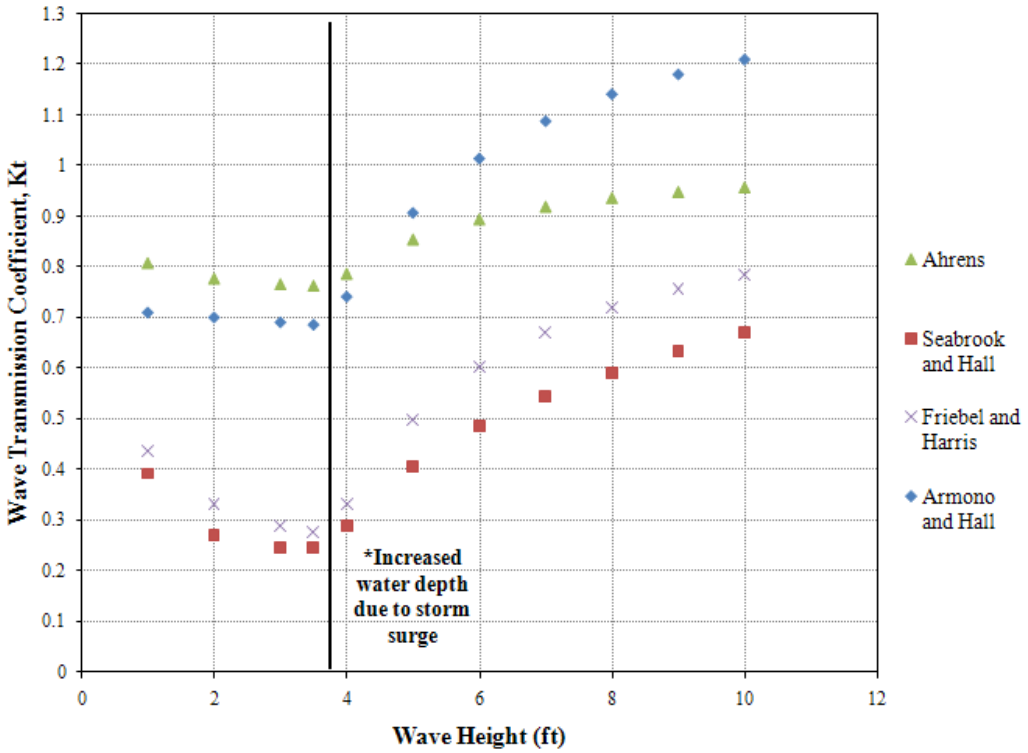

Figure 34. Wave transmission coefficient for a wave period of 10 seconds.

5.5 *Sediment Transport*

The Shields diagram was used to determine the horizontal water particle velocity required for sediment movement. A boundary shear stress of 0.165 lb/ft-s^2 produces a grain Reynolds number and Shields parameter of 6, and 0.04, respectively, shown in Table 14. As shown in Figure 35, this boundary shear stress is required to move the sediment found in front of the Marriott Hotel.

Table 14. Variables calculated to determine when sediment transport occurs.

Variable		Symbol	Units
Boundary shear stress	0.165	τ_o	lb/ft-s^2
Grain Reynolds Number	6	R_*	N/A
Shields parameter	0.04	τ_*	N/A
Velocity	0.91	U	ft/s

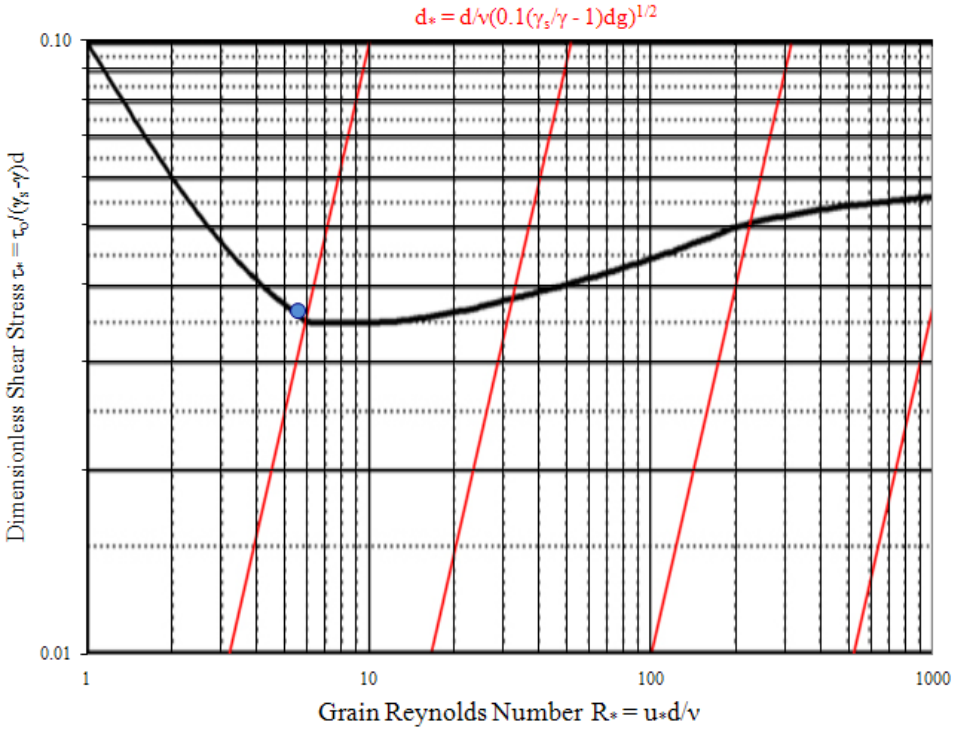

Figure 35. Shields diagram showing variables required for sediment transport.

Using Equation 20, the minimum horizontal velocity required for sediment movement is 0.91 ft/s. The horizontal water particle velocity results from the H_t determined from the Friebel and Harris method were compared to the minimum velocity required for sediment movement. For a wave period of 4 seconds, sediment should not move under non-storm conditions, as seen in Table 15. Bold numbers indicate theoretical sediment movement. Tables 16, 17, and 18 show that sediment should begin to move for a wave height of three feet and a wave period of

6, 8, and 10 seconds respectively. Sediment transport should occur under conditions with storm surge for all cases.

Table 15. Results using Friebel and Harris method for a period of 4 seconds.

H (ft)	**T (s)**	**d (ft)**	**Storm Surge (ft)**	**L (ft)**	**U (ft/s)**	**K_t**	**H' = H*K_t (ft)**	**U' (ft/s)**
1	4	4.8	0	46.67	1.13	0.37	0.37	0.42
2	4	4.8	0	46.67	2.27	0.26	0.53	0.60
3	4	4.8	0	46.67	3.40	0.22	0.66	0.75
3.5	4	4.8	0	46.67	3.97	0.21	0.73	0.82
4	4	5.13	0.33	48.03	4.35	0.26	1.05	**1.15**
5	4	6.41	1.61	52.74	4.68	0.43	2.15	**2.01**
6	4	7.69	2.89	56.73	4.92	0.53	3.20	**2.62**
7	4	8.97	4.17	60.17	5.09	0.60	4.21	**3.06**
8	4	10.26	5.46	63.15	5.21	0.65	5.20	**3.39**
9	4	11.54	6.74	65.73	5.27	0.69	6.17	**3.62**
10	4	12.82	8.02	67.97	5.30	0.71	7.12	**3.77**

Table 16. Results using Friebel and Harris method for a period of 6 seconds.

H (ft)	**T (s)**	**d (ft)**	**Storm Surge (ft)**	**L (ft)**	**U (ft/s)**	**K_t**	**H' = H*K_t (ft)**	**U' (ft/s)**
1	6	4.8	0	72.33	1.23	0.40	0.40	0.49
2	6	4.8	0	72.33	2.45	0.30	0.59	0.72
3	6	4.8	0	72.33	3.68	0.25	0.76	**0.93**
3.5	6	4.8	0	72.33	4.30	0.24	0.83	**1.02**
4	6	5.13	0.33	74.86	4.72	0.29	1.18	**1.39**
5	6	6.41	1.61	83.06	5.19	0.46	2.31	**2.40**
6	6	7.69	2.89	90.29	5.60	0.57	3.39	**3.17**
7	6	8.97	4.17	96.77	5.95	0.63	4.44	**3.78**
8	6	10.26	5.46	102.69	6.25	0.68	5.47	**4.28**
9	6	11.54	6.74	108.06	6.52	0.72	6.48	**4.70**
10	6	12.82	8.02	113.00	6.76	0.75	7.47	**5.05**

Table 17. Results using Friebel and Harris method for a period of 8 seconds.

H (ft)	**T (s)**	**d (ft)**	**Storm Surge (ft)**	**L (ft)**	**U (ft/s)**	**K_t**	**H' = H*K_t (ft)**	**U' (ft/s)**
1	8	4.8	0	97.94	1.26	0.42	0.42	0.53
2	8	4.8	0	97.94	2.51	0.32	0.63	0.79
3	8	4.8	0	97.94	3.77	0.27	0.82	**1.03**
3.5	8	4.8	0	97.94	4.39	0.26	0.91	**1.14**
4	8	5.13	0.33	101.13	5.00	0.32	1.26	**1.58**
5	8	6.41	1.61	112.57	5.90	0.48	2.42	**2.85**
6	8	7.69	2.89	122.80	6.28	0.59	3.52	**3.68**
7	8	8.97	4.17	132.07	6.63	0.66	4.59	**4.35**
8	8	10.26	5.46	140.62	6.96	0.71	5.65	**4.91**
9	8	11.54	6.74	148.50	7.26	0.74	6.68	**5.39**
10	8	12.82	8.02	155.85	7.54	0.77	7.70	**5.80**

Table 18. Results using Friebel and Harris method for a period of 10 seconds.

H (ft)	**T (s)**	**d (ft)**	**Storm Surge (ft)**	**L (ft)**	**U (ft/s)**	**K_t**	**H' = H*K_t (ft)**	**U' (ft/s)**
1	10	4.8	0	123.09	1.27	0.44	0.44	0.55
2	10	4.8	0	123.09	2.54	0.33	0.66	0.84
3	10	4.8	0	123.09	3.81	0.29	0.87	**1.10**
3.5	10	4.8	0	123.09	4.44	0.28	0.96	**1.22**
4	10	5.13	0.33	127.16	4.91	0.33	1.33	**1.63**
5	10	6.41	1.61	141.77	5.46	0.50	2.50	**2.73**
6	10	7.69	2.89	154.87	5.95	0.60	3.62	**3.58**
7	10	8.97	4.17	166.81	6.39	0.67	4.71	**4.30**
8	10	10.26	5.46	177.92	6.79	0.72	5.78	**4.90**
9	10	11.54	6.74	188.19	7.16	0.76	6.83	**5.43**
10	10	12.82	8.02	197.81	7.51	0.79	7.86	**5.90**

6 Conclusions

This study analyzed the performance of a submerged breakwater constructed of Reef Ball artificial reef units. Only few such breakwaters have been constructed, so that studies for this type of submerged breakwater are limited. Monitoring studies are important because they show actual performance in field results that can only be estimated by physical and numerical modeling.

Analysis of the Marriott Reef Ball Breakwater System was accomplished through examining shoreline, cross-shore, and volumetric changes, plus predicted wave transmission. Data included beach profile surveys, aerial images, and beach width measurements.

Prior to installation of the breakwater system, the beach in front of the Marriott Hotel had a serious erosion problem. In addition to long-term erosion, seasonal fluctuations of 50 feet occurred. The beach disappeared with the shoreline retreating to the seawall in November 2002. Following construction of the breakwater, the beach width, profile, and volume of sand significantly increased. The beach continued to experience seasonal fluctuations, with the beach width varying from an average 25 to 70 feet.

The Marriott Reef Ball Breakwater System has successfully modified the wave and current fields landward of the breakwater to induce accretion and beach stability. The breakwater's large width and small freeboard contributed to higher wave attenuation and a greater level of protection. A salient build-up was documented at the southern end of the breakwater. This build-up occurred because Reef Ball units as submerged breakwaters were able to reduce sediment movement leeward of the structure under non-storm conditions. During storm conditions involving elevated water level due to storm surge, the wave heights are not

attenuated enough and will induce sediment movement. Current and wave data were not collected in the monitoring study, but their effects were determined analytically.

7 Recommendations

There are a few recommendations for future studies. Comprehensive monitoring of the study area should be continued to determine the long term effects of the breakwater system. Increasing the spatial domain to include beaches further north and south of the structure should be added to the monitoring studies to examine the impacts of the structure on neighboring beaches. In addition to increasing the spatial domain, increasing the temporal domain would also be beneficial to help document seasonal changes. Also, daily beach width measurements should be re-established by the Marriott Hotel. Wave data measurements should be collected around the breakwater to provide data for wave attenuation determination.

References

Ahrens, J. 1987. *Characteristics of Reef Breakwaters.* Vicksburg, MS: Coastal Engineering Research Center, U.S. Army Corps of Engineers Waterways Experiment Station.

Armono, and Hall, K. 2003. Laboratory study of wave transmission on artifical reefs. *Proceeding of Canadian Coastal Engineering Conference.* Kingston, Canada: Canadian Society for Civil Engineering.

Beach Review and Assessment Committee. 2003. Interim Report.

Birben, A., *et. al.* 2007. Investigation of the effects of offshore breakwater parameters on sediment accumulation. *Ocean Engineering , 34*, 284-302.

Black, K. 2000. Artificial surefing reef for erosion control and amenity: Theory and Application. *International Coastal Symposium.*

Black, K., and Andrews, C. 2001. Sandy shoreline response to offshore obstacles: Part 1. Salient and tombolo geometry and shape. *Journal of Coastal Research , 29* (Special Issue), 82-93.

Black, K., and Mead, S. 2001. Wave rotation for coastal protection. *Proceedings for Coast and Ports 2001-the 15th Australasian Coastal Conference and Ocean Engineering Conference.*

Blanchon, P., and Jones, B. 1997. Hurricane control on shelf-edge-reef architechture around Grand Cayman. *Sedimentology , 44*, 479-506.

Boak, E., and Turner, I. 2005. Shoreline definition and detection: A review. *Journal of Coastal Research , 21*, 688-703.

Dally, W.R., and Pope, J., 1986. Detached breakwaters for shore protection. Technical Report, CERC 86-1.

Darbyshire *et al*., 1976. Results os Investigations into the Oceanography. In:Wickstead, J.H. (ed.), Cayman Islands Natural Resource Study; Part III. U.K. Ministry of Overseas Development, 120 pp.

Dean, R., *et. al.* 1997. Full scale monitoring study of a submerged breakwater, Palm Beach, Florida, USA. *Coastal Engineering , 29*, 291-315.

Dean, R., and Dalrymple, R. 2002. *Coastal Processes with Engineering Applications.* Cambridge: Cabridge University Press, 475 pp.

Douglass, L., and Weggel, J.R., 1987. Performance of a perched Beach-Slaughter Beach, Delaware. *Proceedins Coastal Sediments '87*. ASCE, pp. 1385–1398.

Friebel, H., and Harris, L. 2004. A new wave transmission coefficient model for submerged breakwaters. *Proceedings 29th International Conference on Coastal Engineering.* Lisbon Portugal.

Gorman, L., et. al. 1998. Monitoring the coastal environment; Part IV: Mapping, shoreline changes, and bathymetric analysis. *Journal of Coastal Research, 14*, 61-92.

Hanson, H., and Kraus, N.C. (2001). Chronic beach erosion adjacent to inlets and remediation by composite (T-head) groins. ERDC/CHL CHETN IV-36, U.S. Army Engineer Research and Development Center, Vicksburg, MS.

Harris, L. 1996. *Wave Attenuation by Rigid and Flexible-Membrane Submerged Breakwaters.* Doctoral dissertation, Florida Atlantic University.

Harris, L. 2002. *Marriott Grand Cayman Resort Seawall.* Memo.

Harris, L. 2003a. *Status report for the submerged Reef Ball artifical reef submerged breakwater beach stabilization project for the Grand Cayman Mariott Hotel.*

Harris, L. 2003b. Submerged reef structures for beach erosion control. *Third International Coastal Structures Conference.* Portland, Oregon.

Harris, 2006. Artificial reefs for ecosystem restoration and coastal erosion protection with aquaculture and recreational amenities. *5th International Surfing Reef Conference.*

Komar, P. and Miller, M. 1975. Sediment threshold under oscillatory waves. *Proceedings 14th International Conference Coastal Engineering,* ASCE, 756-775.

Lowe, R. J., *et al*. 2005. Spectral wave dissipation over a barrier reef. *Journal of Geophysical Research*, 110 (Oceans).

Madsen, O.S. and Grant, W. D. 1975. The threshold of sediment movement under oscillatory waves: a discussion. *Journal of Sedimentary Petrology, 45,* 360-361.

Nir, Y., 1982. Offshore artificial structure and their influence on the Israel and Sinai Mediterranean Beaches. *Proceedings of the 18th International Conference on Coastal Engineering*, 1857–1855 pp.

NOAA Coastal Services Center. 2008. Historical Hurricane Tracks. Retrieved May 20th, 2008, from http://maps.csc.noaa.gov/hurricanes/viewer.html

Precht, W. 2006. *Coral Reef Restoration Handbook.* Boca Raton: Taylor and Francis Group, 363 pp.

Pilarczyk, K. 2003. Design of low-crested (submerged) structures –an overview. *Proceedings 6th International Conference on Coastal and Port Engineering in Developing Countries*, 1-18 pp.

Pilarczyk, K., and Zeilder, R.1996. *Offshore Breakwaters and Shore Evolution Control.* A.A. Balkerma, Rotterdam, The Netherlands, 572 pp.

Ranasinghe, R., *et. al.* 2006. Shoreline response to multi-fuctional artifical surfing reefs: A numerical and physical modeling study. *Coastal Engineering , 53,* 259-280.

Ranasinghe, R., and Turner, I. 2006. Shoreline response to submerged structures: A review. *Coastal Engineering , 53*, 65-79.

Reef Ball Company, Ltd. 2007. *Reef Balls as Submerged Breakwaters for Erosion Control.* Retrieved March 15, 2008, from Reef Beach: http://www.reefbeach.com

Roehl, E. 1997. *The Stability of Manufactured Artificial Reefs*, Master's thesis, Florida Institute of Technology.

Rouse, H. 1939. An Analysis of Sediment Transportation in the Light of Fluid Turbulence, Soil Conservation Service Report no. SCS-TP-25, U.S. Department of Agriculture, Washington, D.C.

Schiererck, G. (2001). *Introduction to Bed, Bank, and Shore Protection.* Delft: Delft University Press.

Seabrook S.R. and Hall K.R. 1998. Wave transmission at submerged rubble mound breakwaters. *Proc. 26th International Conference on Coastal Engineering.* Copenhagen.

Sleath, J. 1984. *Sea Bed Mechanics*. New York: John Whiley and Sons, 335 pp.

Shields, A. 1936. *Application of Similarity Principles and Turbulence Research to Bedload Movement,* California Institute of Technology, Pasadena.

Silvester, R. and J.R.C. Hsu. 1997. *Coastal Stabilization*, World Scientific Publishing Co, Singapore, 578 pp.

Stauble, D., and Tabar, J. 2003. The use of submerged narrow-crested breakwaters for shoreline erosion. *Journal of Coastal Research , 19*, 684-722.

Stewart, S. 2005. Tropical Cyclone Report Hurricane Ivan. Retrieved May 15th, 2008, from National Hurricane Center: http://.www.nhc.noaa.gov/2004ivan.html

Suh, K., and Dalrymple, R., 1987. Offshore Breakwaters in Laboratory and Field. *Journal of Waterway, Port, Coastal and Ocean Engineering*, 113, 105–121.

The World Factbook. 2008. *Cayman Islands*. Retrieved April 20, 2008, from http://www.cia.gov/library/publications/the-world-factbook/geos/cj/html

Ting, C., *et. al.* 2004. Porosity effects on non-breaking surface waves over permeable submerged breakwaters. *Coastal Engineering , 50*, 213-224.

U.S. Army Corps of Engineers. 1984. Shore Protection Manual. 4th ed. Vol 2, U. S. Army Engineer Waterways Experiment Station, U.S. Government Printing Office, Wasington, D.C., 1088 pp.

U.S. Army Corps of Engineers. 1995. *Sediment Transport Mechanics.* Engineering and Design-Sedimentation Investigations of Rivers and Reservoir Engineering Manual, Chapter 9.

U.S. Army Corps of Engineers. 2006a. *Types and functions of coastal structures.* Coastal Engineering Manual, Part VI, Chapter 2.

U. S. Army Corps of Engineers, 2006b. *Hydrodynamics of tidal inlets.* Coastal Engineering Manual, Part II, Chapter 6.

Vanoni, V. 1975. *Sedimentation Engineering.* New York: ASCE, 745 pp.

Weaver, D. 2003. The Political Ecologyof Tourism in the Cayman Islands. In S. Gossling, *Tourism and Development in Tropical Islands.* Northampton: Edward Elgar Publishing, Inc.

Young, S. 2004. Impact of Hurricane Ivan in Grand Cayman. Retrieved April 20, 2008, from http://stormcarib.com/reports/2004/SRYCAYMAN.PDF

Yuan, D., and Tao, J. 2003. Wave forces on submerged, alternately submerged, and emerged semicircular breakwaters. *Coastal Engineering , 28*, 75-93.

Appendix A

Storm Information

Table A-19. Storm Information for Grand Cayman Island, 1975-1989.
(NOAA Coastal Services, 2008)

Year	Month	Day	Storm Name	Wind Speed(KTS)	Pressure (MB)	Category
1975	8	26	CAROLINE	25	1012	TD
1975	8	26	CAROLINE	25	1012	TD
1975	9	19	ELOISE	35	1000	TS
1975	9	19	ELOISE	35	1000	TS
1975	9	20	ELOISE	35	1000	TS
1980	8	6	ALLEN	125	955	H4
1980	8	7	ALLEN	135	945	H4
1981	5	7	ARLENE	30	1006	TD
1981	5	7	ARLENE	30	1005	TD
1981	5	7	ARLENE	35	1003	TS
1981	11	3	KATRINA	30	1002	TD
1981	11	4	KATRINA	30	1001	TD
1981	11	4	KATRINA	35	1000	TS
1981	11	4	KATRINA	40	998	TS
1981	11	4	KATRINA	50	996	TS
1981	11	5	KATRINA	60	993	TS
1981	11	5	KATRINA	65	988	H1
1985	8	12	DANNY	25	1010	TD
1985	8	12	DANNY	25	1010	TD
1985	8	12	DANNY	25	1010	TD
1988	9	13	GILBERT	115	952	H4
1988	9	13	GILBERT	125	934	H4
1988	9	13	GILBERT	140	905	H5

Table A-20. Storm Information for Grand Cayman Island, 1990-2007.
(NOAA Coastal Services, 2008)

Year	Month	Day	Storm Name	Wind Speed(KTS)	Pressure (MB)	Category
1995	10	9	ROXANNE	45	999	TS
1995	10	9	ROXANNE	50	995	TS
1996	8	19	DOLLY	25	1009	TD
1996	8	19	DOLLY	30	1008	TD
1996	11	25	MARCO	50	1002	TS
1996	11	25	MARCO	55	1001	TS
2000	9	19	HELENE	30	1010	TD
2000	9	20	HELENE	30	1010	TD
2002	9	19	ISIDORE	50	998	TS
2002	9	19	ISIDORE	50	990	TS
2002	9	19	ISIDORE	60	990	TS
2002	9	19	ISIDORE	65	983	H1
2002	9	20	ISIDORE	75	979	H1
2002	9	30	LILI	65	986	H1
2002	9	30	LILI	65	984	H1
2002	10	1	LILI	70	978	H1
2004	8	12	CHARLEY	75	988	H1
2004	8	12	CHARLEY	80	984	H1
2004	8	12	CHARLEY	90	980	H2
2004	9	12	IVAN	145	910	H5
2004	9	12	IVAN	135	915	H4
2004	9	12	IVAN	135	919	H4
2004	9	12	IVAN	130	920	H4
2004	9	13	IVAN	140	916	H5
2005	7	17	EMILY	140	929	H5
2005	7	17	EMILY	135	940	H4
2005	7	17	EMILY	130	946	H4
2007	8	20	DEAN	130	926	H4
2007	8	20	DEAN	130	926	H4

Appendix B

Tidal Data

The tidal data was used to adjust survey data taken for the surveys conducted from 02/07 to 06/08 to MSL.

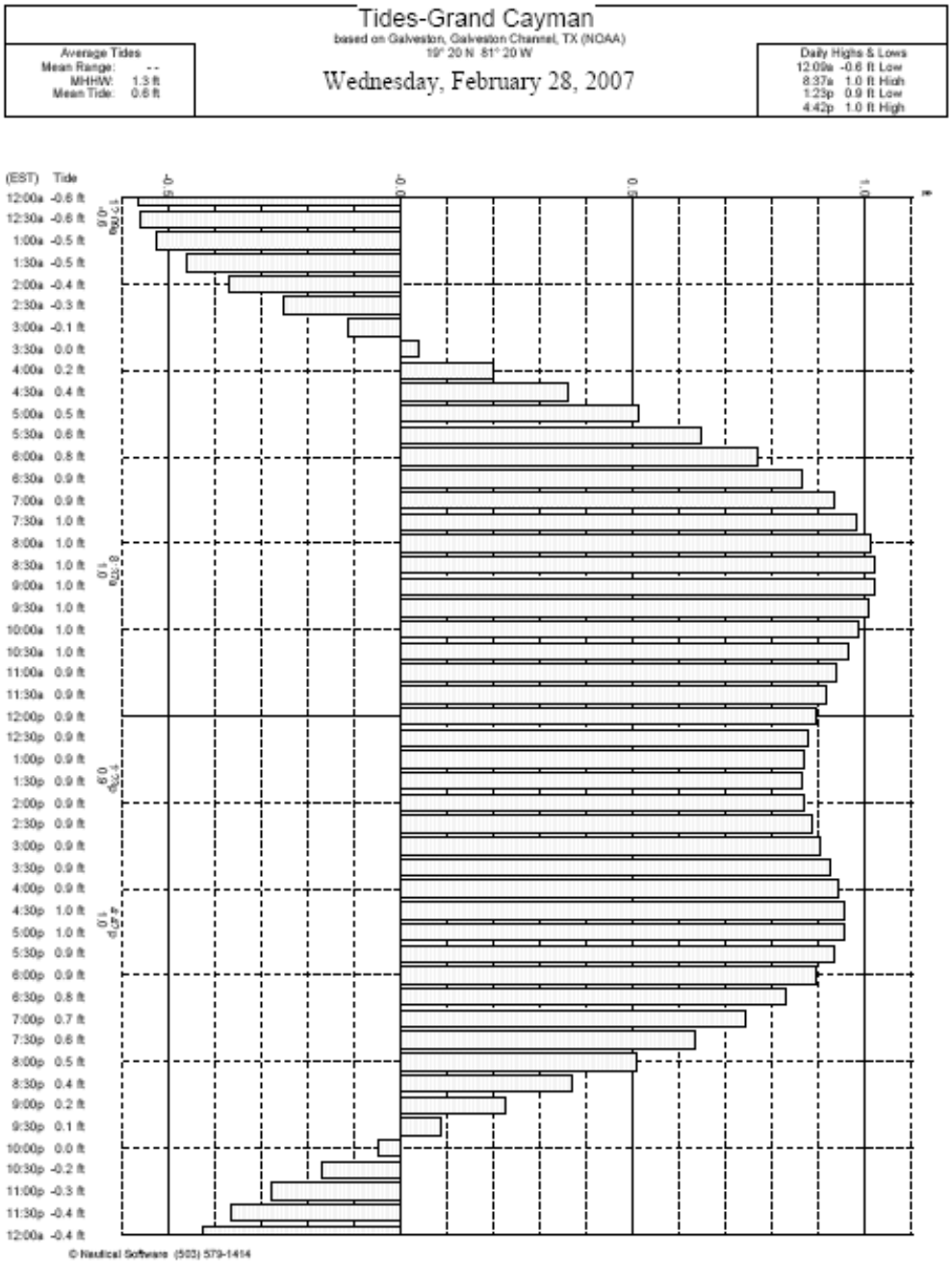

Figure B-1. Tidal Data for 02/28/07.

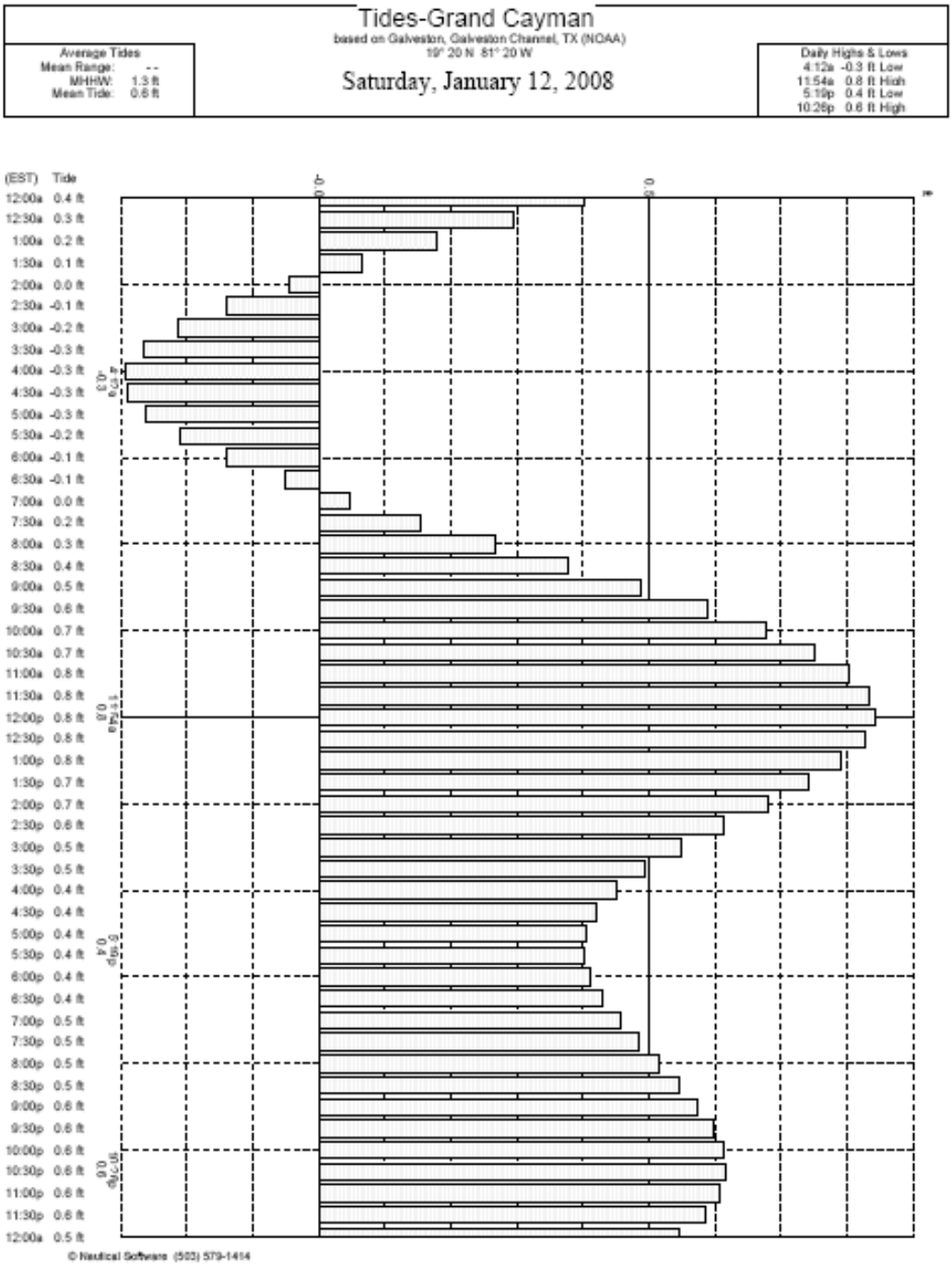

Figure B-2. Tidal Data for 01/1208.

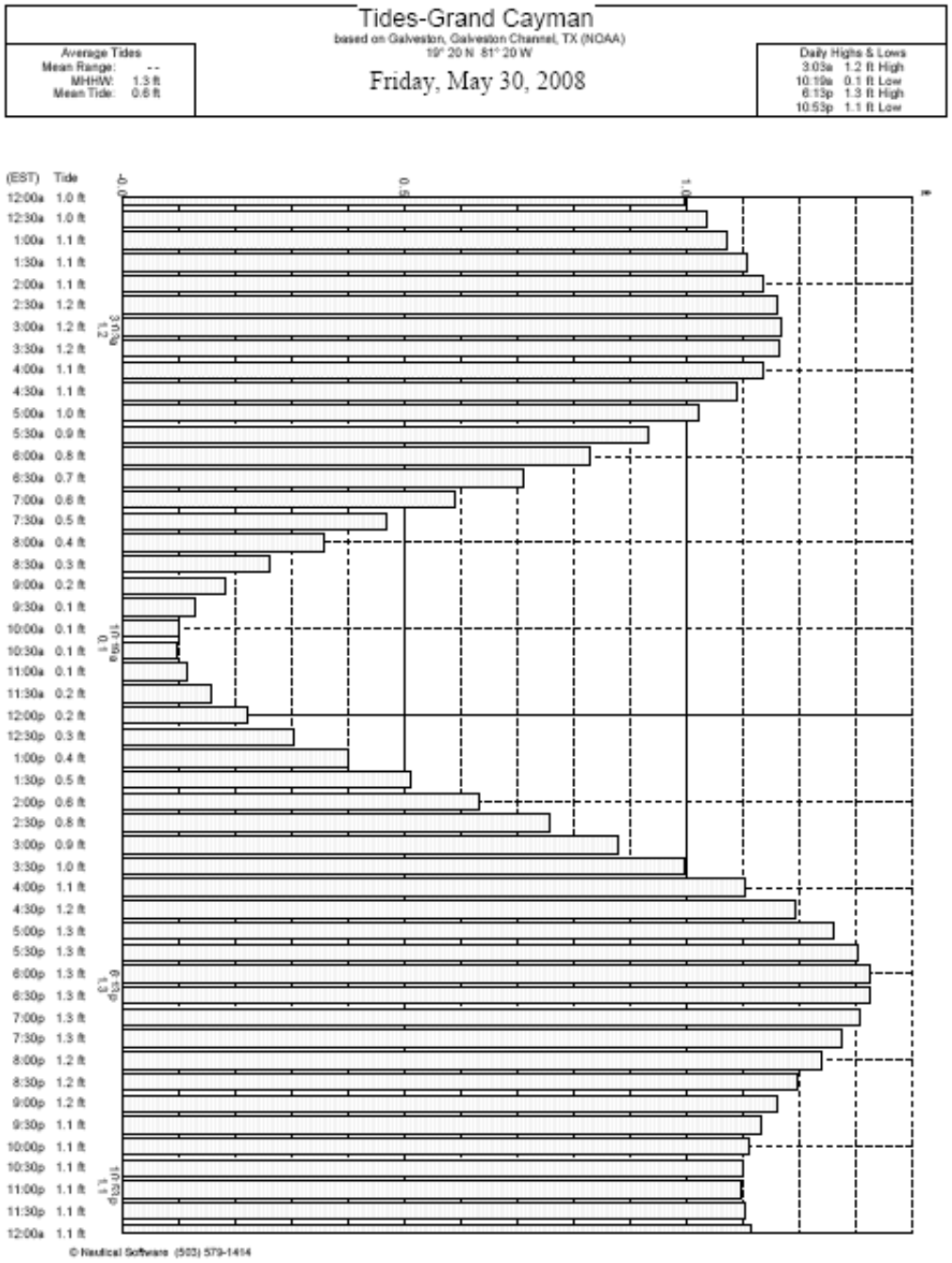

Figure B-3. Tidal Data for 05/30/08.

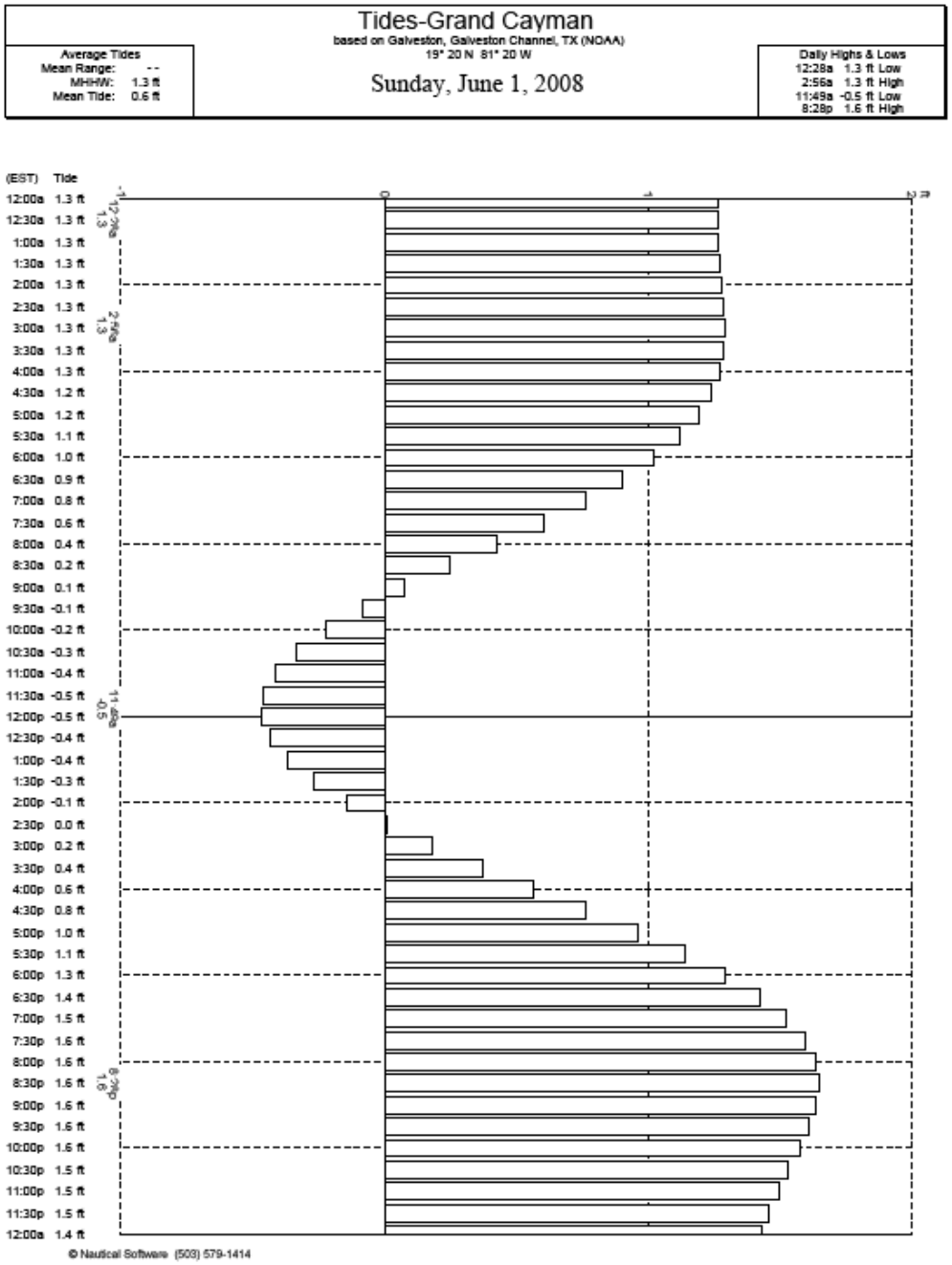

Figure B-4. Tidal Data for 06/01/08.

Appendix C

Photographs

Figure C-1. Aerial photographs for 1972 and 1994
(from right to left)
(Photo Courtesy Tim Austin, Cayman Islands Department of Environment)

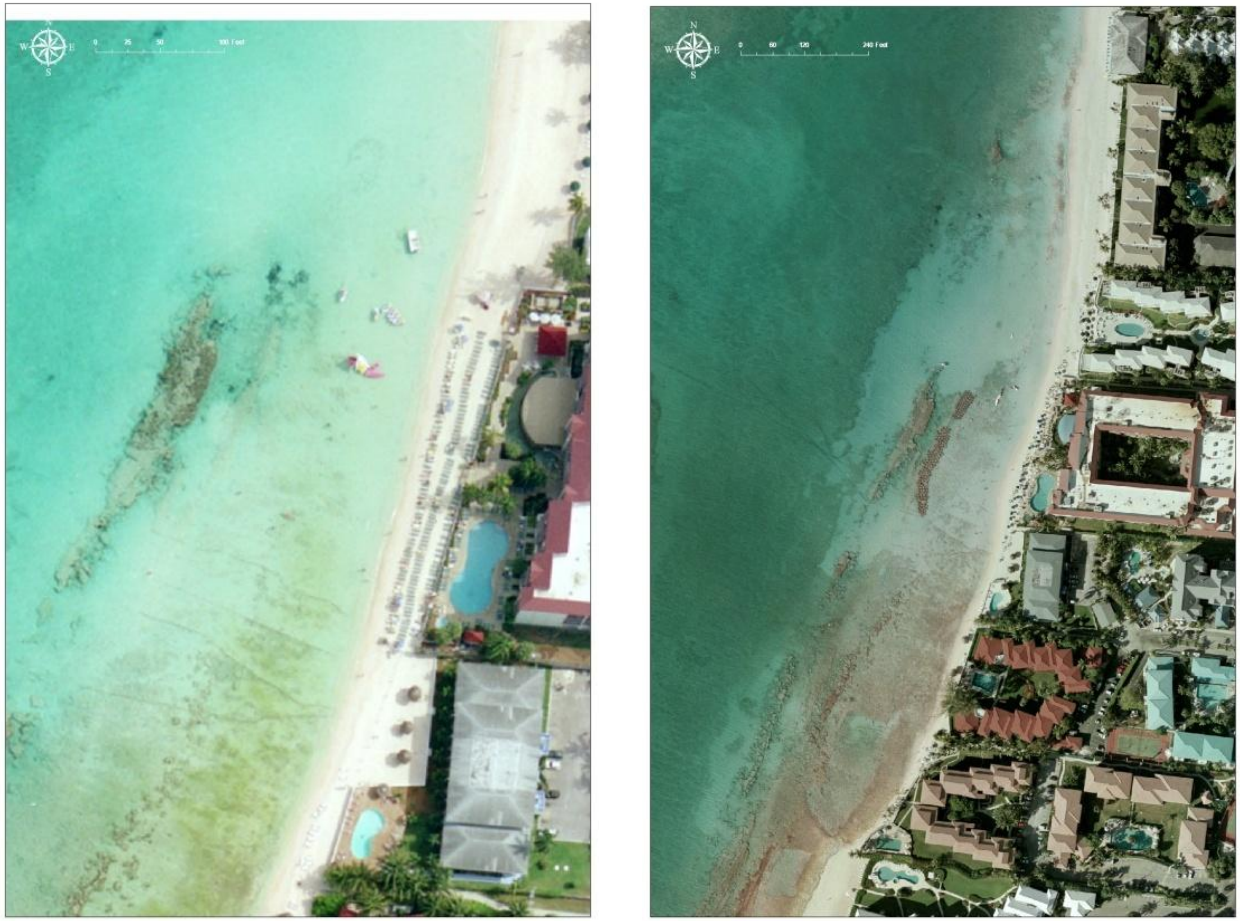

Figure C-2. Aerial photographs for 1999 and 2004 (April)
(from right to left)
(Photo Courtesy Tim Austin, Cayman Islands Department of Environment)

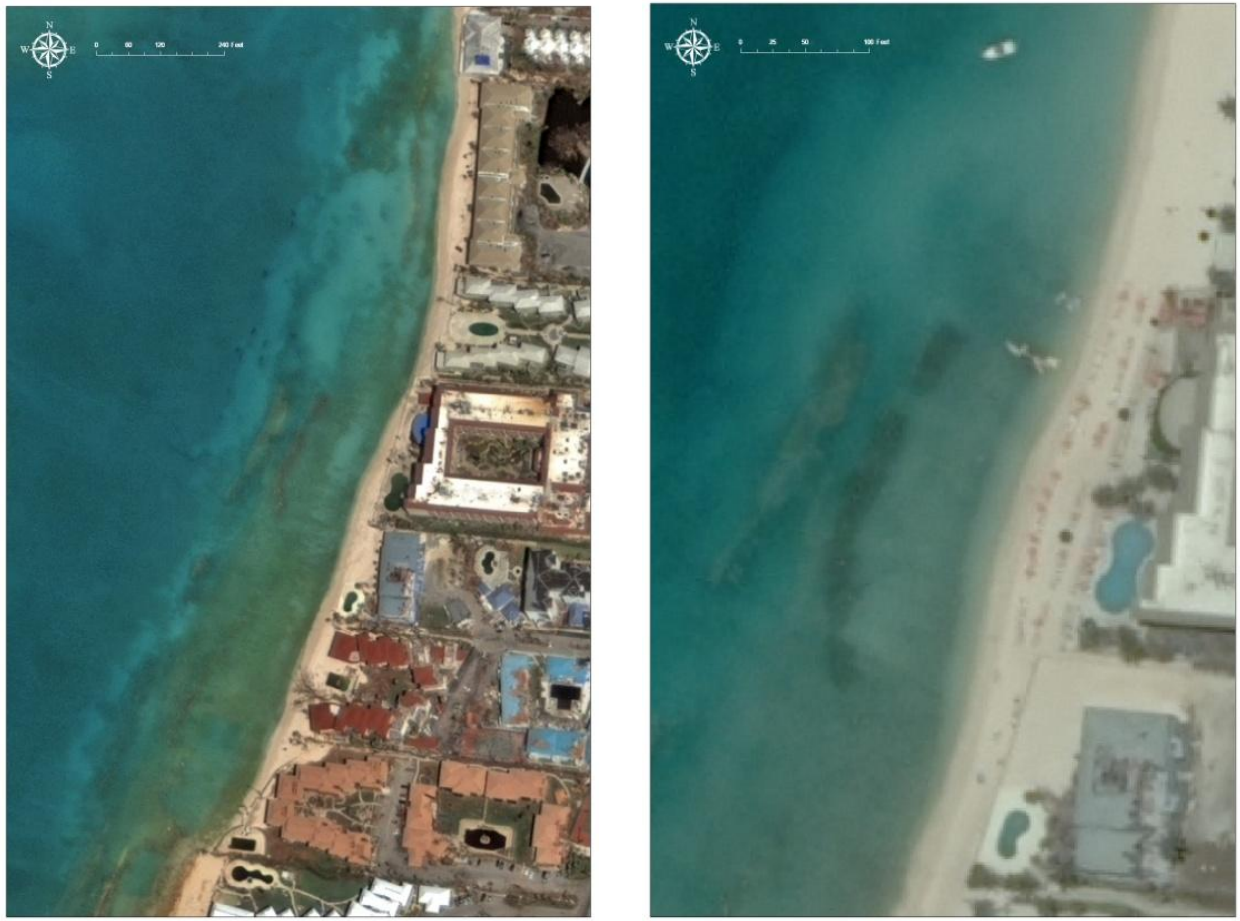

Figure C-3. Aerial photographs for 2004 (Nov.) and 2006.
(from right to left)
(Photo Courtesy Tim Austin, Cayman Islands Department of Environment)

Figure C-4. View looking to the South and North at seawall in Oct. 2002

Figure C-5. View looking to the South and North at seawall in 02/03.

Figure C-6. View looking to the South and North at seawall in May 2005.
(All photographs courtesy of Lee Harris)

Figure C-7. View looking to the South and North at seawall in 01/08.

Figure C-8. View looking to the South and North at seawall in 06/08.

Figure C-9. Example of rocky shoreline to the south (02/03) and boat docking to the north (01/08) of the Marriot Hotel.
(All photographs courtesy of Lee Harris)

Appendix D

Sand Sample Report

QUARRY PRODUCTS LTD

Project Number: Not Applicable
Job Name: Routine Test
Supplier: Hadsphaltic
Material: Beach Sand
Date Sampled: 24th October 2002
Date Tested: 24th October 2002

Sample #: One
Description:Tan Sand with Shell Fragments
Source: Marriott Beach,Grand Cayman
ASTM Test: C 136
By: Ray Howe
By: Tony Fuller

MOISTURE DETERMINATION	MASS
Container Tare (g)	353.9
Tare & Wet Sample (g)	961.5
Tare & Oven Dried Sample (g)	942.9
Loss of Moisture (g)	18.6
Mass of Dry Sample (g)	589.0
Moisture %	3.2

WASH TEST	MASS
Tare & Dry Sample	
Container Tare	
Mass of Dry Sample	
AFTER WASHING & DRYING	
Tare & Washed Sample	
Mass of Washed Sample	
Mass lost (Passing # 200)	
Passing # 200 on Dry Screening	
Total Passing # 200	

DRY SIEVE ANALYSIS					WET SIEVE ANALYSIS			
Sieve Size	Weight Retained (G)	% Retained	% Passing	Spec's	Weight Retained (G)	% Retained	% Passing	Spec's
2	0	0						
1.5	0	0	100.0					
1	0	0.0	100.0					
3/4	0	0.0	100.0					
1/2	0	0.0	100.0					
3/8	0	0.0	100.0					
# 4	3	0.5	99.5					
# 8	1.2	0.2	99.3					
# 16	8.2	1.4	97.9					
# 30	105.7	17.9	79.9					
# 50	395.4	67.1	12.8					
# 100	74.6	12.7	0.1					
# 200	0.2	0.0	0.1					
Pan	0.6	0.1						
Total	588.9							
Difference %	0.001							

The Fineness Modulus of this sample is 2.1

* **Fineness Modulus**: This is an index number which is roughly proportional to the average size of particles in a given aggregate, that is, the coarser the aggregate the higher the Fineness Modulus

Appendix E

Wave Transmission

Table E-1. Design parameters used in determining wave transmission.

Wave Height, H (ft)	d (ft)	F(ft)	F/H	B/d	h/d	F/B
1	4.8	-0.7	-0.70	5.21	0.85	-0.028
2	4.8	-0.7	-0.35	5.21	0.85	-0.028
3	4.8	-0.7	-0.23	5.21	0.85	-0.028
3.5	4.8	-0.7	-0.20	5.21	0.85	-0.028
4	5.13	-1.03	-0.26	4.88	0.80	-0.04
5	6.41	-2.31	-0.46	3.90	0.64	-0.09
6	7.69	-3.59	-0.60	3.25	0.53	-0.14
7	8.97	-4.87	-0.70	2.79	0.46	-0.19
8	10.26	-6.16	-0.77	2.44	0.40	-0.25
9	11.54	-7.44	-0.83	2.17	0.36	-0.30
10	12.82	-8.72	-0.87	1.95	0.32	-0.35

Table E-2. Design parameters used in determining wave transmission.

T (s)	4			6			8			10		
H (ft)	L(ft)	B/L	H_i/gT^2	L(ft)	B/L	H_i/gT^2	L(ft)	B/L	H_i/gT^2	L(ft)	B/L	H_i/gT^2
1	46.67	0.54	0.002	72.33	0.35	0.001	97.94	0.26	0.000	123.09	0.20	0.000
2	46.67	0.54	0.004	72.33	0.35	0.002	97.94	0.26	0.001	123.09	0.20	0.001
3	46.67	0.54	0.006	72.33	0.35	0.003	97.94	0.26	0.001	123.09	0.20	0.001
3.5	46.67	0.54	0.007	72.33	0.35	0.003	97.94	0.26	0.002	123.09	0.20	0.001
4	48.03	0.52	0.008	74.86	0.33	0.003	101.13	0.25	0.002	127.16	0.20	0.001
5	52.74	0.47	0.010	83.06	0.30	0.004	112.57	0.22	0.002	141.77	0.18	0.002
6	56.73	0.44	0.012	90.29	0.28	0.005	122.80	0.20	0.003	154.87	0.16	0.002
7	60.17	0.42	0.014	96.77	0.26	0.006	132.07	0.19	0.003	166.81	0.15	0.002
8	63.15	0.40	0.016	102.69	0.24	0.007	140.62	0.18	0.004	177.92	0.14	0.002
9	65.73	0.38	0.017	108.06	0.23	0.008	148.50	0.17	0.004	188.19	0.13	0.003
10	67.97	0.37	0.019	113.00	0.22	0.009	155.85	0.16	0.005	197.81	0.13	0.003

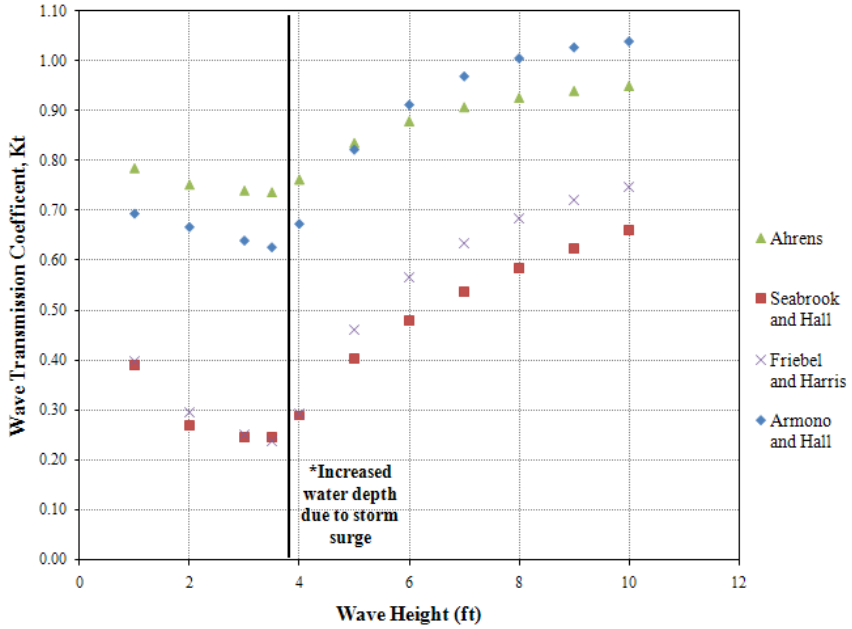

Figure E-1. Wave transmission coefficient between for methods for a wave period of 6 seconds.

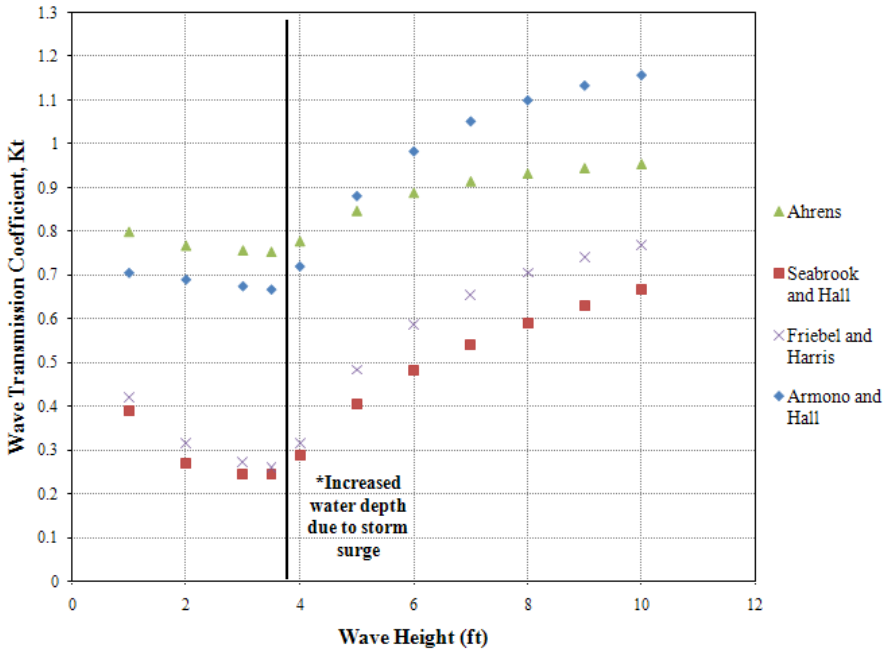

Figure E-2. Wave transmission coefficient between for methods for a wave period of 8 seconds.

Table E-3. Results using Armono and Hall method for a period of 4 seconds.

H (ft)	T (s)	d (ft)	Storm Surge (ft)	L (ft)	U (ft/s)	K_t	H' = H*K_t (ft)	U' (ft/s)
1	4	4.8	0	46.67	1.13	0.66	0.66	0.75
2	4	4.8	0	46.67	2.27	0.60	1.20	1.36
3	4	4.8	0	46.67	3.40	0.54	1.62	1.83
3.5	4	4.8	0	46.67	3.97	0.51	1.78	2.02
4	4	5.13	0.33	48.03	4.35	0.54	2.15	2.34
5	4	6.41	1.61	52.74	4.68	0.65	3.27	3.06
6	4	7.69	2.89	56.73	4.92	0.71	4.26	3.49
7	4	8.97	4.17	60.17	5.09	0.73	5.13	3.73
8	4	10.26	5.46	63.15	5.21	0.74	5.88	3.83
9	4	11.54	6.74	65.73	5.27	0.72	6.51	3.82
10	4	12.82	8.02	67.97	5.30	0.70	7.02	3.72

Table E-4. Results using Armono and Hall method for a period of 6 seconds.

H (ft)	T (s)	d (ft)	Storm Surge (ft)	L (ft)	U (ft/s)	K_t	H' = H*K_t (ft)	U' (ft/s)
1	6	4.8	0	72.33	1.23	0.69	0.69	0.85
2	6	4.8	0	72.33	2.45	0.67	1.33	1.64
3	6	4.8	0	72.33	3.68	0.64	1.92	2.36
3.5	6	4.8	0	72.33	4.30	0.63	2.19	2.69
4	6	5.13	0.33	74.86	4.72	0.67	2.69	3.18
5	6	6.41	1.61	83.06	5.19	0.82	4.11	4.27
6	6	7.69	2.89	90.29	5.60	0.91	5.47	5.11
7	6	8.97	4.17	96.77	5.95	0.97	6.78	5.76
8	6	10.26	5.46	102.69	6.25	1.00	8.04	6.28
9	6	11.54	6.74	108.06	6.52	1.03	9.24	6.70
10	6	12.82	8.02	113.00	6.76	1.04	10.39	7.02

Table E-5. Results using Armono and Hall method for a period of 8 seconds.

H (ft)	T (s)	d (ft)	Storm Surge (ft)	L (ft)	U (ft/s)	K_t	H' = H*K_t (ft)	U' (ft/s)
1	8	4.8	0	97.94	1.26	0.71	0.71	0.89
2	8	4.8	0	97.94	2.51	0.69	1.38	1.73
3	8	4.8	0	97.94	3.77	0.68	2.03	2.54
3.5	8	4.8	0	97.94	4.39	0.67	2.34	2.93
4	8	5.13	0.33	101.13	4.85	0.72	2.88	3.49
5	8	6.41	1.61	112.57	5.37	0.88	4.40	4.73
6	8	7.69	2.89	122.80	5.84	0.98	5.90	5.73
7	8	8.97	4.17	132.07	6.25	1.05	7.36	6.57
8	8	10.26	5.46	140.62	6.62	1.10	8.79	7.28
9	8	11.54	6.74	148.50	6.96	1.13	10.19	7.88
10	8	12.82	8.02	155.85	7.27	1.16	11.57	8.41

Table E-6. Results using Armono and Hall method for a period of 10 seconds.

H (ft)	T (s)	d (ft)	Storm Surge (ft)	L (ft)	U (ft/s)	K_t	H' = H*K_t (ft)	U' (ft/s)
1	10	4.8	0	123.09	1.27	0.71	0.71	0.90
2	10	4.8	0	123.09	2.54	0.70	1.40	1.78
3	10	4.8	0	123.09	3.81	0.69	2.07	2.63
3.5	10	4.8	0	123.09	4.44	0.69	2.40	3.05
4	10	5.13	0.33	127.16	4.91	0.74	2.97	3.64
5	10	6.41	1.61	141.77	5.46	0.91	4.54	4.95
6	10	7.69	2.89	154.87	5.95	1.02	6.09	6.04
7	10	8.97	4.17	166.81	6.39	1.09	7.63	6.96
8	10	10.26	5.46	177.92	6.79	1.14	9.14	7.76
9	10	11.54	6.74	188.19	7.16	1.18	10.64	8.46
10	10	12.82	8.02	197.81	7.51	1.21	12.11	9.09

Table E-7. Results using Seabrook and Hall method for a period of 4 seconds.

H (ft)	T (s)	d (ft)	Storm Surge (ft)	L (ft)	U (ft/s)	K_t	H' = H*K_t (ft)	U' (ft/s)
1	4	4.8	0	46.67	1.13	0.39	0.39	0.44
2	4	4.8	0	46.67	2.27	0.27	0.53	0.61
3	4	4.8	0	46.67	3.40	0.24	0.73	0.83
3.5	4	4.8	0	46.67	3.97	0.24	0.85	0.97
4	4	5.13	0.33	48.03	4.35	0.29	1.15	1.25
5	4	6.41	1.61	52.74	4.68	0.40	2.00	1.87
6	4	7.69	2.89	56.73	4.92	0.47	2.85	2.34
7	4	8.97	4.17	60.17	5.09	0.53	3.71	2.70
8	4	10.26	5.46	63.15	5.21	0.58	4.61	3.00
9	4	11.54	6.74	65.73	5.27	0.61	5.53	3.24
10	4	12.82	8.02	67.97	5.30	0.65	6.50	3.44

Table E-8. Results using Seabrook and Hall method for a period of 6 seconds.

H (ft)	T (s)	d (ft)	Storm Surge (ft)	L (ft)	U (ft/s)	K_t	H' = H*K_t (ft)	U' (ft/s)
1	6	4.8	0	72.33	1.23	0.39	0.39	0.48
2	6	4.8	0	72.33	2.45	0.27	0.54	0.66
3	6	4.8	0	72.33	3.68	0.24	0.73	0.90
3.5	6	4.8	0	72.33	4.30	0.25	0.86	1.05
4	6	5.13	0.33	74.86	4.72	0.29	1.15	1.36
5	6	6.41	1.61	83.06	5.19	0.40	2.02	2.10
6	6	7.69	2.89	90.29	5.60	0.48	2.88	2.69
7	6	8.97	4.17	96.77	5.95	0.54	3.76	3.20
8	6	10.26	5.46	102.69	6.25	0.58	4.68	3.66
9	6	11.54	6.74	108.06	6.52	0.63	5.63	4.08
10	6	12.82	8.02	113.00	6.76	0.66	6.62	4.47

Table E-9. Results using Seabrook and Hall method for a period of 8 seconds.

H (ft)	T (s)	d (ft)	Storm Surge (ft)	L (ft)	U (ft/s)	K_t	H' = H*K_t (ft)	U' (ft/s)
1	8	4.8	0	97.94	1.26	0.39	0.39	0.49
2	8	4.8	0	97.94	2.51	0.27	0.54	0.68
3	8	4.8	0	97.94	3.77	0.25	0.74	0.92
3.5	8	4.8	0	97.94	4.39	0.25	0.86	1.08
4	8	5.13	0.33	101.13	5.00	0.29	1.16	1.45
5	8	6.41	1.61	112.57	5.37	0.41	2.03	2.18
6	8	7.69	2.89	122.80	5.84	0.48	2.90	2.82
7	8	8.97	4.17	132.07	6.25	0.54	3.78	3.38
8	8	10.26	5.46	140.62	6.62	0.59	4.71	3.90
9	8	11.54	6.74	148.50	6.96	0.63	5.67	4.38
10	8	12.82	8.02	155.85	7.27	0.67	6.67	4.85

Table E-10. Results using Seabrook and Hall method for a period of 10 seconds.

H (ft)	T (s)	d (ft)	Storm Surge (ft)	L (ft)	U (ft/s)	K_t	H' = H*K_t (ft)	U' (ft/s)
1	10	4.8	0	123.09	1.27	0.39	0.39	0.50
2	10	4.8	0	123.09	2.54	0.27	0.54	0.68
3	10	4.8	0	123.09	3.81	0.25	0.74	0.94
3.5	10	4.8	0	123.09	4.44	0.25	0.86	1.09
4	10	5.13	0.33	127.16	4.91	0.29	1.16	1.42
5	10	6.41	1.61	141.77	5.46	0.41	2.03	2.22
6	10	7.69	2.89	154.87	5.95	0.48	2.91	2.88
7	10	8.97	4.17	166.81	6.39	0.54	3.80	3.47
8	10	10.26	5.46	177.92	6.79	0.59	4.72	4.01
9	10	11.54	6.74	188.19	7.16	0.63	5.69	4.53
10	10	12.82	8.02	197.81	7.51	0.67	6.70	5.03

Table E-11. Results using Ahrens method for a period of 4 seconds.

H (ft)	T (s)	d (ft)	Storm Surge (ft)	L (ft)	U (ft/s)	K_t	H' = H*K_t (ft)	U' (ft/s)
1	4	4.8	0	46.67	1.13	0.76	0.76	0.87
2	4	4.8	0	46.67	2.27	0.73	1.46	1.65
3	4	4.8	0	46.67	3.40	0.72	2.15	2.44
3.5	4	4.8	0	46.67	3.97	0.71	2.50	2.83
4	4	5.13	0.33	48.03	4.35	0.74	2.96	3.22
5	4	6.41	1.61	52.74	4.68	0.82	4.09	3.82
6	4	7.69	2.89	56.73	4.92	0.87	5.19	4.25
7	4	8.97	4.17	60.17	5.09	0.90	6.27	4.56
8	4	10.26	5.46	63.15	5.21	0.92	7.33	4.77
9	4	11.54	6.74	65.73	5.27	0.93	8.38	4.91
10	4	12.82	8.02	67.97	5.30	0.94	9.42	4.99

Table E-12. Results using Ahrens method for a period of 6 seconds.

H (ft)	T (s)	d (ft)	Storm Surge (ft)	L (ft)	U (ft/s)	K_t	H' = H*K_t (ft)	U' (ft/s)
1	6	4.8	0	72.33	1.23	0.79	0.79	0.96
2	6	4.8	0	72.33	2.45	0.75	1.50	1.85
3	6	4.8	0	72.33	3.68	0.74	2.22	2.73
3.5	6	4.8	0	72.33	4.30	0.74	2.58	3.17
4	6	5.13	0.33	74.86	4.72	0.76	3.05	3.60
5	6	6.41	1.61	83.06	5.19	0.84	4.18	4.34
6	6	7.69	2.89	90.29	5.60	0.88	5.28	4.92
7	6	8.97	4.17	96.77	5.95	0.91	6.35	5.40
8	6	10.26	5.46	102.69	6.25	0.93	7.41	5.79
9	6	11.54	6.74	108.06	6.52	0.94	8.46	6.13
10	6	12.82	8.02	113.00	6.76	0.95	9.49	6.42

Table E-13. Results using Ahrens method for a period of 8 seconds.

H (ft)	T (s)	d (ft)	Storm Surge (ft)	L (ft)	U (ft/s)	K_t	H' = H*K_t (ft)	U' (ft/s)
1	8	4.8	0	97.94	1.26	0.80	0.80	1.00
2	8	4.8	0	97.94	2.51	0.77	1.53	1.93
3	8	4.8	0	97.94	3.77	0.76	2.27	2.85
3.5	8	4.8	0	97.94	4.39	0.75	2.63	3.31
4	8	5.13	0.33	101.13	4.85	0.78	3.11	3.77
5	8	6.41	1.61	112.57	5.37	0.85	4.23	4.55
6	8	7.69	2.89	122.80	5.84	0.89	5.33	5.18
7	8	8.97	4.17	132.07	6.25	0.91	6.40	5.71
8	8	10.26	5.46	140.62	6.62	0.93	7.45	6.17
9	8	11.54	6.74	148.50	6.96	0.94	8.50	6.57
10	8	12.82	8.02	155.85	7.27	0.95	9.53	6.93

Table E-14. Results using Ahrens method for a period of 10 seconds.

H (ft)	T (s)	d (ft)	Storm Surge (ft)	L (ft)	U (ft/s)	K_t	H' = H*K_t (ft)	U' (ft/s)
1	10	4.8	0	123.09	1.27	0.81	0.81	1.03
2	10	4.8	0	123.09	2.54	0.78	1.56	1.98
3	10	4.8	0	123.09	3.81	0.77	2.30	2.92
3.5	10	4.8	0	123.09	4.44	0.76	2.67	3.40
4	10	5.13	0.33	127.16	4.91	0.79	3.15	3.86
5	10	6.41	1.61	141.77	5.46	0.85	4.27	4.66
6	10	7.69	2.89	154.87	5.95	0.89	5.36	5.31
7	10	8.97	4.17	166.81	6.39	0.92	6.43	5.87
8	10	10.26	5.46	177.92	6.79	0.94	7.48	6.35
9	10	11.54	6.74	188.19	7.16	0.95	8.53	6.79
10	10	12.82	8.02	197.81	7.51	0.96	9.56	7.18